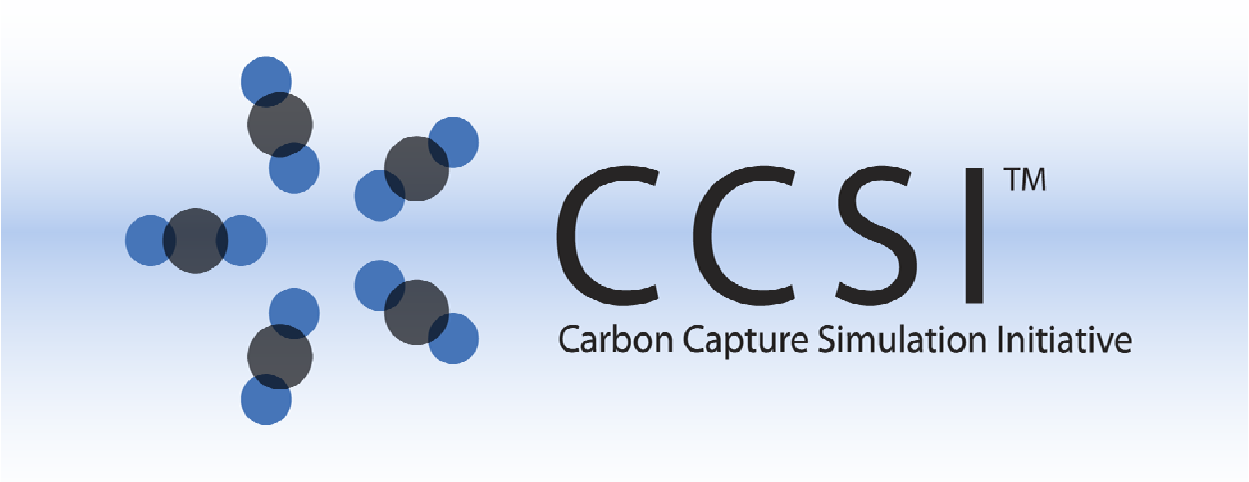

NETL ARRA Report on the Development of a Process Design of a Solid Sorbent Carbon Capture Process

Prepared by
Andrew Lee, Hosoo Kim, Juan Morinelly, John Eslick, and David Miller
National Energy Technology Laboratory
Morgantown, WV 26505

In collaboration with Carnegie Mellon University and Lawrence Livermore National Laboratory

Prepared for

U.S. Department of Energy
National Energy Technology Laboratory

24 February 2012

Revised 30 March 2012

Revision Log

Revision	Date	Revised By:	Description
0	02/24/2012	Andrew Lee, Hosoo Kim, David Miller	Original
1	03/26/2012	Andrew Lee, Hosoo Kim, David Miller	Corrects COE and clarifies some sections
2	4/23/2012	David Miller	Corrects duplicated figure

Disclaimer

Acknowledgement of Funding

This project was funded under the Carbon Capture Simulation Initiative under the following FWP's and contracts:

LANL - FE-101-002-FY10

PNNL - 60115

LLNL - FEW0180

LBNL - CSNW1130

NETL - RES-0004000.6.600.007.002

Table of Contents

1.0 Introduction 5
2.0 Solid Sorbent Based Carbon Capture 6
Solid Sorbent Material 6
Gas-Solid Contacting Reactors 6
3.0 Process Design and Optimization 8
Process Simulation 8
Reactor Models 8
Power Plant Model 8
Compression Model 10
Miscellaneous Equipment Models 11
Optimization Framework 11
Objective Function and Constraints 12
Cost Estimation 14
4.0 Process Description 15
5.0 Process Economics 21
6.0 Process Analysis 22
7.0 Conclusions 24
8.0 Glossary 25
9.0 References 26
Appendix A: Bubbling Fluidized Bed Reactor Model 27
Assumptions 28
Model Equations 29
Kinetic Model 29
Appendix B: Moving Bed Reactor Model 31
Assumptions 31
Model Equations 32
Appendix C: Costing Methodology and Models 36
Appendix D: Specification Sheets 41

List of Figures

Figure 3-1. Optimization framework and procedure..... 12
Figure 4-1. Process flow diagram for simulation based optimal design..... 16
Figure 6-1. Cost contributions to COE increase..... 22
Figure A-1. Diagram showing interaction between different regions in a bubbling fluidized bed..... 27
Figure A-2. Flow diagram for an arbitrary slice within the bed..... 28
Figure B-1. Schematic diagram of moving bed reactor. 31

List of Tables

Table 3-1. Flue gas conditions entering carbon capture process. 10
Table 3-2. List of input variables and bounds used in optimization. 13
Table 4-1. Stream table for simulation based optimal design 17
Table 4-2. Major equipment list for simulation based optimal design 20
Table 5-1. Cost Summary 21
Table 5-2. Performance and COE Summary 21
Table 6-1. Enthalpy flows in adsorber and regenerator 23
Table 6-2. Comparison of regeneration energy 23
Table C-1. Daily rates and unit costs for consumables. 39
Table C-2. Parameters for costing methodology. 39
Table C-3. Variables for costing methodology. 40

1.0 Introduction

The goal of the U.S. Department of Energy's Carbon Capture Simulation Initiative (CCSI) is to develop a suite of computational tools that can be deployed to industry to accelerate the development of carbon capture technologies. This report presents the results of the work conducted by the Process Synthesis and Design Team (Task Set 3) during ARRA-funded first year (Feb. 2011 – Jan 2012) of the Carbon Capture Simulation Initiative. A set of computational tools and models for the synthesis and design of solid sorbent based carbon capture processes were developed, and the capabilities of these tools were demonstrated through the design and optimization of an initial full scale design (A650.1) of a solid sorbent capture system for a 650 MWe,net (before capture) supercritical pulverized coal (PC) power plant, which captures 90% of the CO_2 emissions. The tools described in this report include the following:

- An initial set of 1-D process models of solid sorbent adsorbers and regenerators. These are flexible, modular process models of carbon capture equipment that can be used to facilitate the rapid screening of new concepts and technologies.
- An initial heterogeneous simulation-based process optimization framework. This optimization capability allows potential designs to be integrated with the whole power generation system, PC plant, capture process and compression system.

This report also describes how these computation tools were applied to develop and optimize the integrated capture process. Since the resulting process itself will be the basis for subsequent activities within CCSI, it is described in detail. The carbon capture process uses a combination of two-stage bubbling bed adsorbers and moving bed regenerators. The captured CO_2 is compressed to 2220 psia and cooled to 140°F for pipeline transport for subsequent utilization or storage.

2.0 Solid Sorbent Based Carbon Capture

The current state-of-the-art technology for removing CO_2 from gas streams utilizes liquid amine scrubbing technology and is currently commercially available. However, the economic impact of adding amine-scrubbing technologies to power plants is significant, with predicted increase in the cost of electricity of up to 75% (Haslbeck *et al.* [1]). The high costs of liquid amine scrubbing are due to the relatively low loading of CO_2 achieved in the amine solvent and the high heat capacity of the largely aqueous solvent mixture. This results in a very high energy requirement in order to regenerate the solvent. Solid sorbents have been proposed as an alternative to solvent-based scrubbing with the potential to significantly decrease the increase in cost of electricity. In comparison to aqueous amine scrubbing, solid sorbents have a significantly lower specific heat capacity which reduces the amount of heat required for regeneration. They may also be able to achieve higher loadings of CO_2, thus reducing the amount of sorbent material required in the process.

Solid Sorbent Material

A number of different solid materials have been studied as potential sorbents for CO_2, including zeolites, perovskites, activated carbon, carbonates, zirconates and silicates. One of the most promising types of sorbents is those in which an amine is impregnated into or grafted onto a solid substrate. These sorbents combine the efficient CO_2 uptake of liquid amines with the lower heat capacity and high loadings of solid sorbents. A large number of different amine based sorbents have been developed and significant efforts are underway to improve their performance.

For purposes of demonstrating the design capabilities of the CCSI Toolset, NETL sorbent 32D was selected for use as the design basis. NETL 32D has shown a combination of rapid uptake and high loadings of CO_2 at equilibrium under simulated process conditions. Since the sorbent was developed at NETL, the team has full access to experimental information for developing kinetic and equilibrium models of its behavior (Lee *et al.* [2]). NETL 32D is a mixture of polyethyleneimine (PEI) and aminosilanes impregnated into the mesoporous structure of a silica substrate. CO_2 removal is achieved through chemical reactions between the amine sites within the sorbent and the gaseous CO_2 resulting in the formation of solid species bound within the sorbent.

Gas-Solid Contacting Reactors

Among the most significant challenges for implementing solid sorbent-based processes is determining equipment configurations that allow efficient adsorption and regeneration of the sorbent. Gas-solids contacting is a complicated field, and many different processes exist to contact gas and solids under a wide range of conditions. However, few processes exist to process the large volumes of gas containing a relatively low concentration of the active species (CO_2) that are found in power plant flue gases.

Gas-solids contacting equipment can be grouped into four broad categories based on the way the gas and solids move through the system. These categories are 1) fixed beds, 2) moving beds, 3) bubbling fluidized beds, and 4) circulating fluidized beds. Each category of gas-solids contactor has its advantages and disadvantages, and all but moving beds have been successfully used in industrial applications.

Fixed bed contactors consist of a stationary bed of solids through which the gas is passed. Due to the fact that the solid bed is stationary, fixed bed contactors are mechanically simple as they do not need equipment to handle moving solids. However, the fixed bed of solids also necessitates a batch process, as it is necessary to cycle between adsorption and desorption in each bed. This requires more complicated operation and control procedures and also adds an additional energy penalty since the entire reactor vessel must be alternately heated and cooled as opposed to just the solids. Heat and mass transfer within fixed beds is also problematic, as diffusion and conduction are the dominant mechanisms, which results in significant resistance to heat and mass transfer. This makes temperature control within large beds

problematic and can result in the formation of hot spots within the reactor where the temperature is significantly different the rest of the bed. Due to this, fixed bed reactors are often small in order to minimize these effects, thus requiring large numbers of reactors to process a large volume of gas.

Moving bed reactors are similar to fixed bed reactors, except that the solids are gradually moved through the reactor by withdrawing solids from the bottom of the vessel and feeding fresh material at the top. This overcomes the need to operate in batch mode, improving process efficiency. Moving bed reactors still suffer from the heat and mass transfer limitations of fixed beds; however, they are the only form of gas-solids contactor that can achieve true counter-current contacting. This is important for carbon capture processes where the final concentration of the reacting gas (CO_2) is extremely low. By utilizing counter-current contacting, the depleted gas with very low levels of CO_2 is brought into contact with the freshly regenerated sorbent, maximizing the driving force and helping to remove the final amounts of CO_2. Moving bed reactors also have a similar potential advantage for regenerating the sorbent. Due to their potential advantages over fixed bed reactors, moving beds have attracted interest from industry on a number of occasions. However, technical difficulties have thus far prevented their adoption. The main problem with moving bed reactors lies in moving the solids around the system and in the high levels of attrition suffered by the solids. Recent advances in moving bed design (Knaebel [3]) may offer a solution to some of these problems making moving bed contactors an option for solid sorbent based carbon capture.

Fluidized bed reactors, both bubbling and circulating, have been used extensively in a wide range of industrial applications, including fluidized catalytic cracking (FCC) and combustion applications. Fluidized bed reactors operate by passing the gas through the bed of solids at a velocity high enough that the drag forces acting on the particles equals or exceeds the force due to gravity, referred to as the minimum fluidization velocity. Bubbling fluidized beds operate at gas velocities above the minimum fluidization velocity but below the point where all the solids in the bed become entrained by the gas. In this regime, the solids exist as a well defined bed consisting of an emulsion of gas and solids, through which bubbles of gas continuously rise. The flow of gas through the bed is relatively uniform, whilst the solids are well mixed by the action of the bubbles passing through the bed. Bubbling fluidized beds show excellent heat and mass transfer, both within the bed and between the bed and heat exchanger surfaces, due to the well mixed behavior of the bed and good contacting between gas and solids. However, the constant mixing action in the bed can also cause significant attrition of particles and erosion of the reactor vessel and internals. Thus, care must be taken when designing a reactor to address these issues.

Circulating fluidized bed reactors operate at higher gas velocities, above the point where the solids become entrained in the gas. In these systems, the solids are fully entrained and are carried with the gas is a relatively dispersed mixture. The high gas velocities required to entrain the solids allow circulating fluidized beds to process large amounts of gas in relatively small units; however, gas-solids contacting is not as good as in the denser, bubbling fluidized beds. Also, as the solids are entrained in the high velocity gas flow, contacting between gas and solids is co-current which reduces efficiency, and the residence times within even very tall reactors is very short. Circulating fluidized bed reactors also suffer from significant attrition and erosion effects, especially near the gas and solids outlet at the top of the reactor.

Due to the various advantages and disadvantages of the different types of gas-solids contacting equipments, moving bed reactors and bubbling fluidized bed reactors were identified as the most promising types of gas-solid contactors for solid sorbent based carbon capture. Preliminary simulations confirmed the anticipated performance benefits of bubbling bed and moving bed systems. Fixed beds were eliminated due to the difficulties in controlling temperature within the reactor and the issues associated with batch operations. Circulating fluidized beds were eliminated due to their co-current contacting behavior and low residence times, which severely limit their performance for carbon capture operations.

3.0 Process Design and Optimization

In the simulation based optimization approach, it is necessary to first determine the process topology. This process topology was determined based on preliminary results from a superstructure based process synthesis approach. It is a hybrid process utilizing bubbling fluidized bed reactors for the adsorption stage and moving bed reactors for the regeneration stage. Bubbling fluidized bed reactors have good heat and mass transfer characteristics and ability to process large volumes of gas. However, due to the well mixed behavior of the fluidized bed, it is not possible to achieve the desired 90% removal of CO_2 within a single stage. Thus, two beds in counter current series were identified. For regeneration, a moving bed reactor was identified. It can achieve very high levels of regeneration due to its counter-current flow behavior and the ability to inject pure steam at the bottom of the bed to aid in regeneration.

Due to the very large volume of flue gas produced by the power plant, it is not possible to conduct the carbon capture process using a single train of adsorbers and regenerators. There is a maximum practical size for the adsorbers and regenerators, based on the mechanical requirements for constructing the reactor vessels. For the purposes of this study, the upper limit on the size of the adsorber and regenerators columns was restricted to a diameter of 10m, which was based on the size of the largest similar process units currently used in industry. Thus, the design process allows for a number of parallel adsorber and regenerator trains.

In addition to the adsorbers and regenerators, the process also includes compressors for the incoming flue gas, gas-liquid heat exchangers to control the temperature of the incoming flue gas and product gas and cross-over heat solid-liquid heat exchangers to recover heat from the hot sorbent leaving the regenerator. The process also requires solids handling equipment such as elevators and gas-solids separators. Although included in the design, they were not explicitly modeled in the process simulation.

Process Simulation

Reactor Models

Based on the analysis of available gas-solids contacting equipment, detailed models were developed for the two most promising technologies, moving bed reactors and bubbling fluidized bed reactors. These models were developed so as to capture sufficient detail of the behavior to provide accurate and predictive results while remaining computationally tractable. In order to be used for process synthesis and development, the models must be able to produce accurate predictions of the behavior of a given reactor over a wide range of operating conditions and geometries without the need for experimental data to tune the model parameters. However, in order to be useful for optimization the models must also be solvable in a short period of time to allow for multiple evaluations.

To meet these competing requirements, the models developed as part of Task Set 3 are one-dimensional models based on systems of partial differential equations. The use of one dimensional models neglects any radial variations that may occur within the reactors due to maldistribution of gas and solids or wall effects and significantly decreases the computational complexity of the models compared to two- or three-dimensional models such as those developed by Task Set 2. The systems of partial differential equations used in the models address the hydrodynamic behavior, interactions of the gas and solids, the heat and mass transfer phenomena, and the kinetics of the adsorption and desorption reactions. More detailed descriptions of the models and the equations and assumptions involved in developing them are available in Appendices A and B.

Power Plant Model

The addition of a carbon capture process to an existing power plant requires changes to be made to the power plant, due to the additional demands of the capture process. The most significant of these changes

is due to the requirement to draw steam out of the power plant turbine cycle to operate the sorbent regenerators, which results in a derating of the power plant. Due to these interactions between the power plant and the carbon capture process, it is necessary to model the entire plant together in order to properly assess the performance of the system.

A model for a generic 650 MWe,net (before capture) supercritical pulverized coal power plant was developed using SteamPro and Thermoflex modeling software (Thermoflow Inc.). SteamPro is a commercially available software package designed specifically for modeling power plants and is widely used in the power industry. SteamPro includes a set of default designs for different types of power plant equipment (such as boilers, turbines and feedwater heaters) which allow users to rapidly develop models of different types of power plants. These models can then be imported into Thermoflex, which provides more detailed calculations of process behavior and allows for simulation of off-design conditions, which is important for modeling the effects of steam withdrawal from the turbines.

Using the power plant model developed in Thermoflex, a series of simulations were conducted to study the effects of extracting steam from the cross-over between the intermediate and low pressure turbines on the power output. Based on these simulations, a correlation was developed between the rate of steam extraction, F_{steam} (in lb/s), and the new power output from the power plant (before capture, P_{bc} (in kWe), which is shown in Equation 3-1. The required process water, F_{pw} (in lb/s), which varies with the rate of steam extraction, is shown in Equation 3-12.

Equation 3-1. Power plant net power output correlation.

$$P_{bc} = 650,300 - 420.42 F_{steam}$$

Equation 3-2. Process water requirement correlation.

$$F_{pw} = 9.1217 \times 10^{-5} \times F_{steam}{}^{2} - 0.75957 \times F_{steam} + 679$$

These correlations are for steam provided at 100 psia. As shown in Figure 3-1, the parasitic power loss is dependent on the required extracted steam pressure. Whilst the sorbent process requires steam at 100 psia,a CCSI developed simulation of an MEA solvent process requires steam at only 35 psia. When extracting 380 lb/s of steam, for example, 50MW more power is lost when extracting steam at the higher pressure.

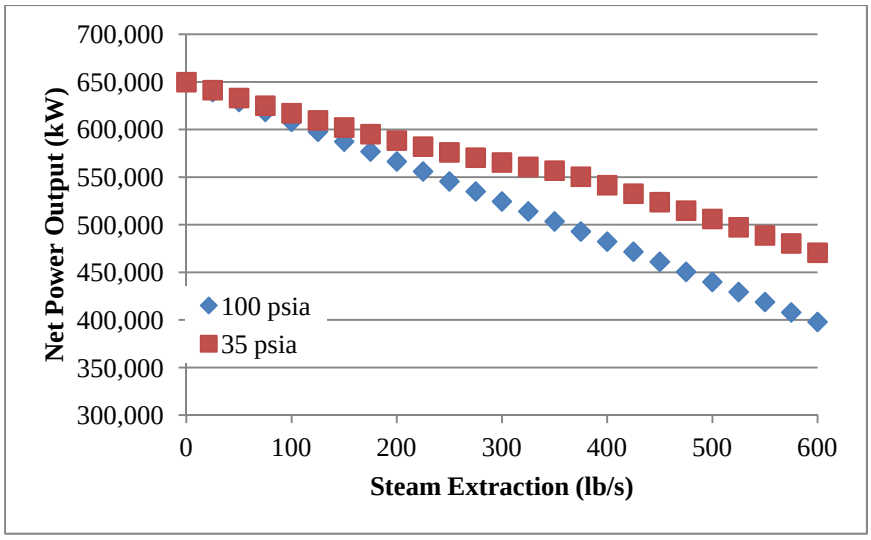

Figure 3-1 Net Power as a Function of Steam Extraction at IP/LP Crossover.

The simulated results from the power plant model were also used to provide the composition and flowrate of the flue gas leaving the FGD unit in the existing plant, which is where the carbon capture process will be integrated into the system. This stream information is shown in Table 3-1.

Table 3-1. Flue gas conditions entering carbon capture process.

Flow Rate	1721.2 lb/s
Pressure	14.683 psi,a
Temperature	129.52°F
CO_2	11.77 mol%
H_2O	14.17 mol%
Other	74.06 mol%

Compression Model

It is also necessary to simulate the compression system required to compress the separated CO_2 to the desired conditions (2200 psi,a and 140°F) in order to determine the amount of power required, which further derates the existing PC plant. Due to the physical properties of gaseous CO_2, the achievable compression ratio in a single compressor stage is very low (less than 2). Thus, a large number of compression stages are needed in order to perform the compression. A detailed model for each compressor stage was developed based on the work of Aungier [4] and used to develop a model for the full CO_2 compression train, including intercoolers. This model was used to predict the electrical power required by the compression process based on the conditions of the separated CO_2 stream from the carbon capture unit and included in the calculation of COE.

Miscellaneous Equipment Models

In order to determine the necessary size, and hence cost, of the ancillary process equipment required for the carbon capture process, simple models for these units were developed and included in the process model. The equipment modeled in this way includes the flue gas blowers and heat exchangers, the product CO_2 cooler, cross-over solid-liquid heat exchangers and pumps for the heat exchanger fluid.

The blowers required to raise the pressure of the incoming flue gas to overcome the pressure drop in the adsorbers were modeled as polytropic compressors using standard design calculations from Seider *et al.* [5]. A polytropic efficiency of 0.85 and mechanical efficiency of 0.97 were assumed for the blowers.

The gas-liquid heats exchangers (flue gas and CO_2 coolers) were modeled as simple single pass counter-current heat exchangers. Cooling water was used as the heat exchange fluid with an initial temperature of 33°C and a final temperature of 45°C. A heat transfer coefficient of 250 $W/m^2.K$ was assumed, and an oversize factor of 1.15 was used to determine the necessary heat transfer area.

The solid-liquid heat exchangers were modeled in a similar way to the gas-liquid heat exchangers, assuming ideal single pass counter-current flow. Pressurized water was used as the heat transfer fluid, which was vaporized using heat from the hot sorbent leaving the regenerator and condensed through heat transfer to the cool sorbent entering the regenerator. A pump and a compressor were provided to move the heat exchanger fluid between the two heat exchanger units. These were sized using design correlations for Seider *et al.* [5].

Additional process equipment, such as the solid elevators and cyclones, were not considered in the process model, but were included in the economic analysis of the process. The cost of these units was estimated based on the flow rates and dimensions of other pieces of process equipment.

Optimization Framework

Optimization of the process was performed using the commercial software package modeFRONTIER™ (ESTECO s.r.l) which communicated with the Aspen Custom Modeler® process model via a Sinter interface linked to Excel, which include all the economic costing modules, as depicted Figure 3-2 (a). A standard simulation interface (sinter) linking an Excel worksheet with Aspen models transfers input information to Aspen Custom Modeler, runs the simulation, and retrieves the results [6]. The optimal design was derived by simulation based optimization using two derivative-free algorithms; the NSGA-II algorithm (Deb *et al.* [7]) and the SIMPLEX algorithm (an implementation of the Nelder-Mead method).

The optimization was conducted in three steps as described in Figure 3-2 (b). A preliminary optimization was carried out using the NSGA-II algorithm for all design variables across the initial variable bounds. The results of this optimization were used to define a reduced set of variable bounds, by the selection of good designs from the initial optimization, which were used in a second optimization procedure using the NSGA-II algorithm. Finally, the optimal solution obtained in the second optimization round was refined using the SIMPLEX algorithm to focus in on the minima.

For the first investigation, an initial population of 300 samples (about 15 times the number of input variables) was generated using uniform Latin hypercube sampling to give good coverage of the parameter space, and the NSGA-II algorithm was run for 10 generations. For the second optimization, an initial population of 300 samples was generated using uniform Latin hypercube sampling within the reduced variable bounds, where the infeasible and unfavorable regimes were removed based on the prior results. The NSGA-II algorithm was run for 20 generations using the new sample set to ensure good convergence on the optimal solution. The obtained solution was further optimized by expanding and contracting the simplex algorithm until the stopping criterion was met. In this optimization, an absolute tolerance of 1E-5 and a maximum of 500 evaluations were used.

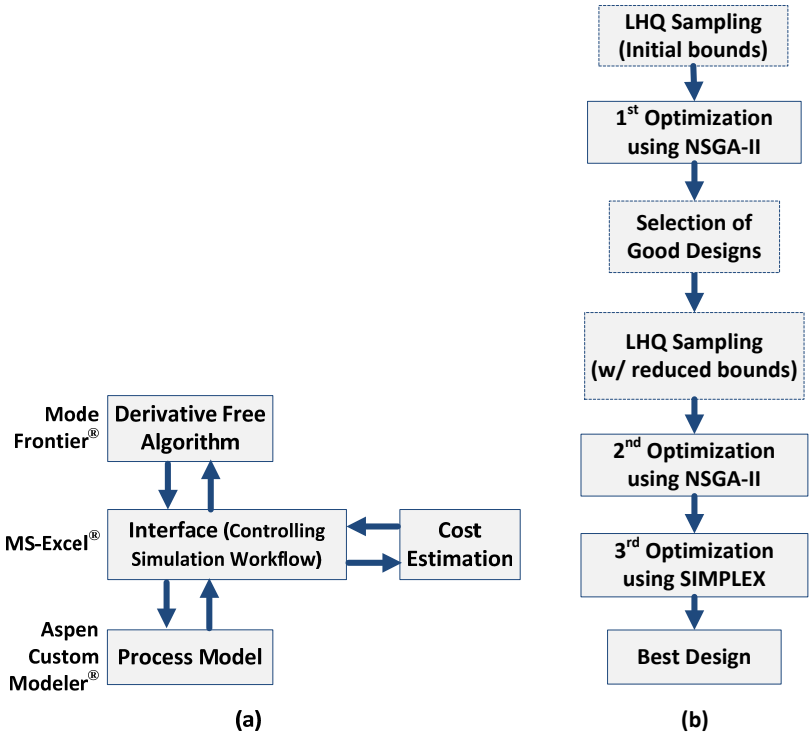

Figure 3-2. Optimization framework and procedure

Objective Function and Constraints

There are a number of possible indicators that can be used when assessing the performance of a power generation system with carbon capture. These indicators can be economic, technical, or environmental in nature. The performance of a process is usually evaluated simultaneously with respect to multiple objectives. The data required for a comprehensive assessment includes capital and operating costs, net power output, and CO_2 emissions. This data is in turn affected by intrinsic assumptions of a particular study such as fuel type, location of the power plant, available financing structure, and many other distinctive features for a given system.

Based on targets specified by NETL, Cost of Electricity (COE) was the primary criterion used to assess the solid sorbent capture process. According to the latest power plant cost estimation methodology published by NETL (Black *et al.* [8]), the COE is "*the revenue received by the generator per net megawatt-hour during the power plant's first year of operation*". Capital and operating costs were estimated based on the specifications of the process, and a detailed costing methodology is provided in Appendix C.

Whilst the fraction of CO_2 capture from the flue gas and the COE of a process are the primary performance indicators, there are a number of additional performance indicators which offer insight into the efficiency of a solid sorbent based carbon capture process. One of these indicators is the loading of CO_2 achieved on the sorbent at different points in the process. The loading of CO_2 is defined as the number of moles of gaseous CO_2 adsorbed per kilogram of sorbent within the process. This can be compared to the predicted equilibrium loading of CO_2 under the same conditions, which gives an indication of the maximum loading of CO_2 that could potentially be achieved under the same conditions.

Another important performance indicator is the working capacity the sorbent, which is defined as the difference between the achieved loading of CO_2 leaving the adsorber and the achieved loading leaving the

regenerator. The working capacity indicates the amount of CO_2 being removed from the flue gas stream per kilogram of sorbent circulated. Processes utilizing sorbents with a high working capacity will be able to remove the same amount of CO_2 with lower circulation rates of sorbent. An equilibrium working capacity can also be calculated as the difference between the predicted equilibrium loading at the outlet to the adsorber and the outlet to the regenerator, which indicates the maximum achievable working load for the conditions used in the process.

Caution should be used when comparing achieved and equilibrium loadings however, as calculation of equilibrium loadings does not take into account the kinetics of the adsorption and desorption reactions. In many cases, solid sorbents show very rapid initial uptake of CO_2, but also have a very long period of slow uptake until they finally reach equilibrium. This period of slow uptake can result in a significant increase in the predicted equilibrium loading of the sorbent. However, due to very slow kinetics this additional loading is unlikely to be achieved in practice. It is also possible to calculate loadings and working capacities for other species that may be adsorbed by the sorbent, such as water. These indicate the extent to which undesired side reactions add to the energy penalty of the process and potentially occupy CO_2 adsorption sites.

A final performance metric for carbon capture processes is the parasitic energy requirement of the process. The parasitic energy requirement is the amount of power drawn from the power plant to operate the carbon capture process. The parasitic energy requirement of a carbon capture process can generally be attributed to two main sources: energy lost due to extraction of steam from the power plant steam cycle and electrical power required to run process equipment. Solid sorbent based carbon capture processes generally require a source of heat in order to regenerate the sorbent, which is normally supplied by extracting steam from the power plant steam cycle. This reduces the flow rate of steam through some of the power plant turbines, reducing the electrical power generated. Carbon capture processes also require electrical power to operate equipment such as pumps, compressors, blowers and solid elevators.

The process was optimized on the basis of minimizing the estimated cost of electricity for the power plant with carbon capture and compression. The primary constraint is the requirement that the process achieve a minimum of 90% removal of carbon dioxide from the incoming flue gas stream.

In addition, there are physical constraints on the size and behavior of the process. Most of these constraints are contained within the bounds placed on the input variables for the optimization; however, the following additional constraints were also considered. First, the gas velocity within the fluidized bed adsorbers must remain within the bubbling or turbulent fluidization regime in order for the reactor model to be applicable. Second, the minimum temperature approach in the solid heat exchanger was enforced.

Table 3-2 lists the input variables to the process model considered in the optimization process, along with the upper and lower bounds placed on these variables. These variables describe the design and operating conditions of all the major process components contained within the carbon capture process.

Table 3-2. List of input variables and bounds used in optimization.

Input Variable	Lower Bound	Upper Bound
Number of Parallel Adsorbers	10	16
Adsorber Diameter (m)	7	10
Top & Bottom Adsorber Bed Depth (m)	4	10
Top & Bottom Adsorber Heat Exchanger Tube Diameter (m)	0.01	0.05
Top & Bottom Adsorber Heat Exchanger Tube Pitch (m)	0.1	0.2
Top & Bottom Adsorber Cooling Water Flowrate (kmol/hr)	30000	60000
Sorbent Flowrate per Adsorber (kg/hr)	350000	600000
Gas Pre-Cooler Temperature (ºC)	40	60
Number of Parallel Regenerators	8	12
Regenerator Height (m)	3	7
Regenerator Diameter (m)	6	10

Regenerator Heat Exchanger Tube Diameter (m)	0.01	0.05
Regenerator Voidage Fraction	0.6	0.9
Regenerator Direct Steam Injection Rate (kmol/hr)	900	1400
Regenerator Heat Exchanger Steam Flowrate (kmol/hr)	2500	5000
Heat Recovery Fluid Flowrate (kmol/hr)	200	700

Cost Estimation

The capital cost of the required process equipment was estimated as the sum of the costs of the 650 MWe,net power plant, carbon capture system and CO_2 compression system. The capital cost of the power plant was obtained based extrapolation of results from recent NETL studies based on net output [1, 8] and from cost estimations from the Thermoflex software package. The capital cost of the CO_2 compression system was estimated based on the power requirement of the compression system, at a cost of $700 per Hp. The capital cost of the carbon capture process equipment was estimated using cost correlations from Seider et al. [5], multiplied by a Lang factor and adjusted for delivery and inflation. These correlations, while useful for estimating relative costs, have a very large absolute uncertainty. Thus, the cost estimates in this report should be viewed as very preliminary estimates. The initial capital cost of the sorbent required for the carbon capture process was also estimated based on a cost of sorbent of $5/lb and the predicted holdup of sorbent within the process. Operating and maintenance costs for the process were estimated based on data from recent NETL studies [1, 8]. A more detailed discussion of the cost estimation process used in Task Set 3 is given in Appendix C.

4.0 Process Description

The process flow diagram of the sorbent-based capture system is depicted in Figure 4-1. A 2-stage bubbling fluidized bed reactor and a moving bed reactor are used for adsorber and regenerator, respectively. The flue gas stream, 1, that is coming from power plant is assumed to comprise carbon dioxide (CO_2), water (H_2O), and nitrogen (N_2). The flowrate, compositions, and thermodynamic conditions are calculated by the power plant model, as shown in Table 3-1. Before being introduced into the adsorber, ADS-001, the flue gas stream is compressed, CPR-001, to meet conditions required for the feed of adsorber. The compressed flue gas stream, 2, is cooled with cooling water, 3, in the GHX-001 where condensate, 6, which comprises condensed water vapor, may be removed. The cooled flue gas stream, 4, passes into ADS-001 through a gas distributor and a CO_2-depleted gas stream, 11, produced via gas-solid contacting is sent to stack.

The fresh sorbent stream, S1 is introduced to the top of ADS-001 and adsorbs CO_2 and H_2O from the flue gas, yielding the loaded sorbent stream, S2. The flowrate of fresh sorbent for each adsorber is calculated by dividing total regenerated sorbent flowrate by number of adsorber units. In the adsorber, sorbent is cooled to remove heat generated by the exothermic adsorption reaction. Cooling is obtained via thermal contact with water cooled heat exchange tubes.

All the loaded sorbent streams are conveyed by a solid moving systems, ELE-001, e.g., a bucket elevator, pneumatic conveyor, or some other means, and are divided into the parallel regeneration units. The sorbent heated by heat-exchanging with recovered heat from hot sorbent at the bottom of regenerator, RGN-001. The sorbent stream for each unit, S3, is partially heated via thermal contact with heat-exchange surface in the SHX-001, the opposite side of which is in contact with saturated steam, 15, which has been vaporized from saturated liquid, 17, by the hot adsorbent via thermal contact with heat-exchange surface in the SHX-002, and which is circulated between the two heat exchangers by small compressor, CPR-002, and pump, CPP-002. The pre-heated sorbent stream, S4, achieves full heating, corresponding temperature, via thermal contact with in-reactor heat exchanging tubes as described in the previous section.

In the tube side of RGN-001, hot steam, 12, extracted at the LP/IP crossover in the power plant turbines is used as a heat source. The effect of heating causes adsorbed species to be desorbed yielding a regenerated sorbent. In addition, a mild condition steam, 14, is also injected at the bottom of reactor to enhance desorption of CO_2 by reducing the mole fraction of CO_2. The injected steam and desorbed species are drawn through the gas collector in stream, 19, at the top of RGN-001 and passes through additional gas water cooled heat exchanger, GHX-002, to condense water vapor, 23, before being carried into the compression train, CPT-001. The CO_2-rich product gas is compressed for pipeline transportation. Finally, the hot regenerated sorbent, S5, leaving the bottom of RGN-001 is partially cooled in heat exchanger, SHX-002, and is delivered again to the top of the adsorber by ELE-002.

This system consists of 14 parallel adsorption units and 10 parallel regeneration units. Stream data and information of major pieces of equipment for the optimal process are shown in Table 4-1 and Table 4-2.

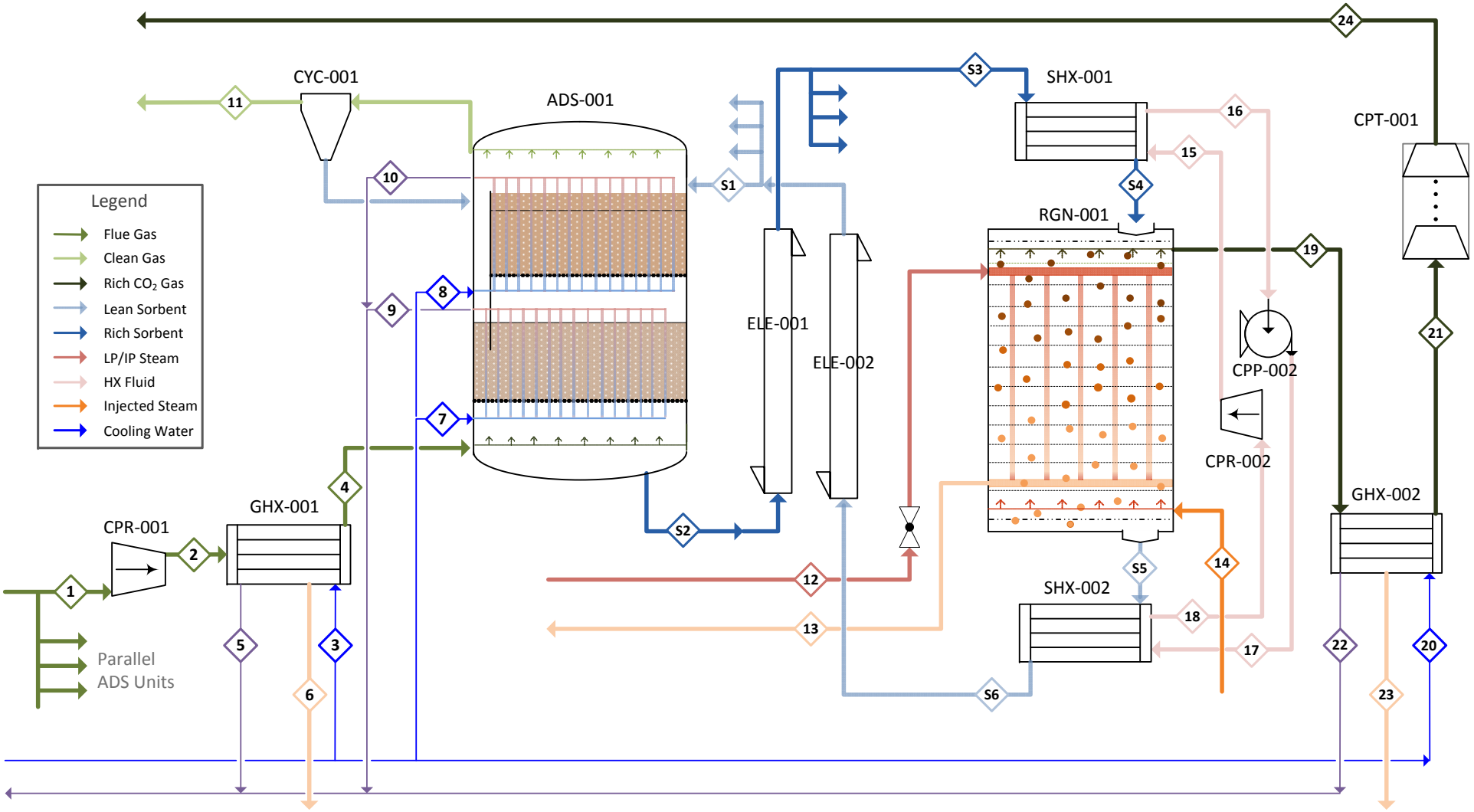

Figure 4-1. Process flow diagram for simulation based optimal design

Table 4-1. Stream table for simulation based optimal design

	1	2	3	4	5	6	7	8	9	10
V-L Mole Fraction										
CO2	0.1177	0.1177	0	0.1291	0	0	0	0	0	0
H2O	0.1417	0.1417	1	0.0587	1	1	1	1	1	1
N2	0.7406	0.7406	0	0.8122	0	0	0	0	0	0
Total	1	1	1	1	1	1	1	1	1	1
Solids Mole Loading (mol/kg)										
Bicarbonate	0	0	0	0	0	0	0	0	0	0
Carbamate	0	0	0	0	0	0	0	0	0	0
H2O	0	0	0	0	0	0	0	0	0	0
Total	0	0	0	0	0	0	0	0	0	0
V-L Flowrate (kmol/hr)	7170	7170	16353	6538	16353	632	45427	47363	45427	47363
V-L Flowrate (kg/hr)	204268	204268	294595	192883	294595	11385	818373	853250	818373	853250
Solids Flowrate (kg/hr)	0	0	0	0	0	0	0	0	0	0
Temperature (°C)	54.18	80.65	33.00	42.88	60.65	42.88	32.20	32.20	42.23	46.50
Pressure (bar)	1.01	1.29	1.00	1.29	1.00	1.29	1.00	1.00	1.00	1.00
Enthalpy (GJ/kmol)	-7.97E-02	-7.89E-02	-2.87E-01	-6.45E-02	-2.85E-01	-2.86E-01	-2.87E-01	-2.87E-01	-2.86E-01	-2.86E-01
Density (kg/m3)	1.06	1.25	844.14	1.45	827.51	838.40	844.60	844.60	838.78	836.23
V-L Molecular Weight	28.49	28.49	18.02	29.50	18.02	18.02	18.02	18.02	18.02	18.02
V-L Flowrate (lbmol/hr)	15807	15807	36051	14414	36051	1393	100149	104417	100149	104417
V-L Flowrate (lb/hr)	450337	450337	649474	425236	649474	25100	1804214	1881104	1804214	1881104
Solids Flowrate (lb/hr)	0	0	0	0	0	0	0	0	0	0
Temperature (°F)	129.52	177.16	91.40	109.18	141.16	109.18	89.96	89.96	108.02	115.71
Pressure (psia)	14.68	18.74	14.50	18.74	14.50	18.74	14.50	14.50	14.50	14.50
Enthalpy (Btu/lbmol)	-3.56E+04	-3.53E+04	-1.28E+05	-2.88E+04	-1.27E+05	-1.28E+05	-1.28E+05	-1.28E+05	-1.28E+05	-1.28E+05
Density (lb/ft3)	0.07	0.08	52.70	0.09	51.66	52.34	52.73	52.73	52.36	52.20

	11	12	13	14	15	16	17	18	19	20
V-L Mole Fraction										
CO2	0.0152	0	0	0.0000	0	0	0	0	0.4196	0
H2O	0.0196	1	1	0.9999	1	1	1	1	0.5803	1
N2	0.9652	0	0	0.0001	0	0	0	0	0.0000	0
Total	1	1	1	1	1	1	1	1	1	1
Solids Mole Loading (mol/kg)										
Bicarbonate	0	0	0	0	0	0	0	0	0	0
Carbamate	0	0	0	0	0	0	0	0	0	0
H2O	0	0	0	0	0	0	0	0	0	0
Total	0	0	0	0	0	0	0	0	0	0
V-L Flowrate (kmol/hr)	5502	3444	3444	1132	270	270	270	270	2537	41276
V-L Flowrate (kg/hr)	154381	62051	62051	20398	4857	4857	4857	4857	73470	743599
Solids Flowrate (kg/hr)	0	0	0	0	0	0	0	0	0	0
Temperature (°C)	51.57	165.11	164.72	105.00	127.89	111.35	111.35	111.35	72.65	33.00
Pressure (bar)	1.00	6.89	6.79	1.86	1.50	1.30	1.50	1.30	1.01	1.20
Enthalpy (GJ/kmol)	-9.94E-03	-2.37E-01	-2.76E-01	-2.39E-01	-2.38E-01	-2.80E-01	-2.80E-01	-2.39E-01	-3.04E-01	-2.87E-01
Density (kg/m3)	1.04	3.55	746.00	1.08	778.87	792.07	792.08	792.07	1.03	844.15
V-L Molecular Weight	28.06	18.02	18.02	18.02	18.02	18.02	18.02	18.02	28.96	18.02
V-L Flowrate (lbmol/hr)	12129	7594	7594	2496	594	594	594	594	5593	90998
V-L Flowrate (lb/hr)	340353	136801	136801	44971	10708	10708	10708	10708	161974	1639363
Solids Flowrate (lb/hr)	0	0	0	0	0	0	0	0	0	0
Temperature (°F)	124.82	329.20	328.49	221.00	262.20	232.43	232.43	232.43	162.78	91.40
Pressure (psia)	14.50	99.97	98.52	27.00	21.75	18.85	21.75	18.85	14.69	17.40
Enthalpy (Btu/lbmol)	-4.45E+03	-1.06E+05	-1.23E+05	-1.07E+05	-1.07E+05	-1.25E+05	-1.25E+05	-1.07E+05	-1.36E+05	-1.28E+05
Density (lb/ft3)	0.06	0.22	46.57	0.07	48.62	49.45	49.45	49.45	0.06	52.70

	21	22	23	24	S1	S2	S3	S4	S5	S6
V-L Mole Fraction										
CO2	0.9358	0	0	0.9951	0	0	0	0	0	0
H2O	0.0641	1	1	0.0048	0	0	0	0	0	0
N2	0.0001	0	0	0.0001	0	0	0	0	0	0
Total	1	1	1	1	0	0	0	0	0	0
Solids Mole Loading (mol/kg)										
Bicarbonate	0	0	0	0	0.1227	0.2004	0.2004	0.2004	0.1227	0.1227
Carbamate	0	0	0	0	0.2298	1.9436	1.9436	1.9436	0.2298	0.2298
H2O	0	0	0	0	0.5118	1.0842	1.0842	1.0842	0.5118	0.5118
Total	0	0	0	0	0.8643	3.2282	3.2282	3.2282	0.8643	0.8643
V-L Flowrate (kmol/hr)	1138	41276	1399	1070	0	0	0	0	0	0
V-L Flowrate (kg/hr)	48259	743599	25211	47039	0	0	0	0	0	0
Solids Flowrate (kg/hr)	0	0	0	0	424451	424451	594231	594231	594231	594231
Temperature (°C)	40.00	52.65	40.00	60.00	118.45	53.89	53.89	69.16	134.66	118.45
Pressure (bar)	1.01	1.10	1.01	153.00	1.01	1.01	1.01	1.01	1.01	1.01
Enthalpy (GJ/kmol)	-3.30E-01	-2.85E-01	-2.86E-01	-4.00E-01	-	-	-	-	-	-
Density (kg/m3)	1.65	832.50	840.10	576.32	-	-	-	-	-	-
V-L Molecular Weight	42.43	18.02	18.02	43.97	-	-	-	-	-	-
V-L Flowrate (lbmol/hr)	2508	90998	3085	2359	0	0	0	0	0	0
V-L Flowrate (lb/hr)	106393	1639363	55580	103704	0	0	0	0	0	0
Solids Flowrate (lb/hr)	0	0	0	0	935758	935758	1310062	1310062	1310062	1310062
Temperature (°F)	104.00	126.78	104.00	140.00	245.21	129.01	129.01	156.49	274.39	245.21
Pressure (psia)	14.68	15.95	14.68	2218.50	14.69	14.69	14.69	14.69	14.69	14.69
Enthalpy (Btu/lbmol)	-1.47E+05	-1.28E+05	-1.28E+05	-1.79E+05	-	-	-	-	-	-
Density (lb/ft3)	0.10	51.97	52.45	35.98	-	-	-	-	-	-

Table 4-2. Major equipment list for simulation based optimal design

	ADS-001A	ADS-001B
Diameter (m)	9.748	
Bed Depth (m)	7.232	4.854
Total HX Area (m2)	1733.7	941.3
Tube Diameter (m)	0.011	0.010
N of Tube	6906	6168
Avg. Bed Voidage	0.569	0.577
Superficial Gas Velocity (m/s)	0.524 ~ 0.558	0.511 ~ 0.508

	RGN-001
Diameter (m)	7.147
Height (m)	4.592
N of Stage	22.959
Total HX Area (m2)	1573.1
Tube Diameter (m)	0.011
N of Tube	10295
Avg. Bed Voidage	4.592
Superficial Gas Velocity (m/s)	0.133 ~ 0.506
Superficial Solid Velocity (m/s)	0.0095

	GHX-001	GHX-002	SHX-001	SHX-002
Total HX Area (m2)	2845.123	5912.363	180.808	759.979
Number of Units	3	7	1	1
Tube-side	Flue Gas	Product Gas	Sat. Steam	Sat. Steam
Inlet Temperature (°C)	80.65	72.65	127.89	111.35
Outlet Temperature (°C)	42.88	40.00	111.35	111.35
Shell-side	Cooling Water	Cooling Water	Solids	Solids
Inlet Temperature (°C)	33.00	33.00	53.89	134.66
Outlet Temperature (°C)	60.65	52.65	69.16	118.45

	CPR-001	CPR-002	CPP-002
Total Power (kW)	1666.519	42.000	0.021
Number of Units	3	1	1
Inlet Pressure (bar)	1.01	1.30	1.30
Outlet Pressure (bar)	1.29	1.50	1.50

5.0 Process Economics

A summary of the cost estimates for the optimized process is given in Table 5-1 and Table 5-2. The cost data used for comparing relative costs is obtained from the benchmark MEA process developed by the CCSI Process Synthesis and Design Team [6], which is calculated on the same cost basis as this sorbent process. The total capital cost of installing the carbon capture and compression process was estimated to be $608M (2007 basis), and the net power output of the retrofitted power plant to be 410.29 MWe,net.

The estimated purchase cost of each adsorption and regeneration section is $3.27M/unit and $1.76M/unit (2007$). 159.62 MWe of derating resulted from steam extracted from the power plant turbines (67%), 54.96 MWe was due to the power demand for the carbon dioxide compression train (23%) and 25.13 MWe was due to the parasitic power demand of the components of the carbon capture process (10%).

The estimated cost of electricity for the power plant with carbon capture and compression was $145.09/MWh (2007$), which represents an increase of 145% in the cost of electricity over the power plant without capture. Note that these are preliminary estimates useful for comparing relative costs of design options using the same methodology. These are not rigorous cost estimates and should not be used for absolute comparisons. In addition, the design basis for this plant uses cooling water at 90°F instead of 60°F as in the NETL Baseline Report [1], which magnifies the effects of the carbon capture retrofit.

Table 5-1. Cost Summary

$1,000, 2007$	Sorbent Process	Benchmark MEA Process
Capital Cost per ADS Unit	$3,266 (1/14 trains)	$4,929 (1/7 trains)
Capital Cost per RGN Unit	$1.759 (1/10 trains)	$4,914 (1/7 trains)
Total Capital Cost	$1,961,927	$2,004,174
Power Plant	$1,316,192	$1,316,192
Hybrid Capture System	$335,037	$465,452
Compression System	$273,040	$220,416
Initial Adsorbent	$37,657	$2,113
Fixed Annual O&M Cost	$53,558	$54,528
Variable Annual O&M Cost	$56,788	$33,936
Annual Fuel Cost	$70,082	$70,082

Table 5-2. Performance and COE Summary

	Sorbent Process	MEA Process	
Net Power Output (MW)	410.29	454.78	MW
CO2 Compression	54.96	44.37	MW
Hybrid System	25.13	8.34	MW
Steam Extraction	159.62	142.81	MW
COE before capture retrofit	59.10	59.10	$/MWh
COE w/ Capture	**138.69**	120.21	$/MWh
COE for TS&M	6.40	5.78	$/MWh
Total COE w/ Capture	**145.09**	125.99	$/MWh

6.0 Process Analysis

Figure 6-1 represents the contribution of different factors to the increase in COE. The effects of parasitic power losses due to steam extraction, CO_2 compression and capture system account for 58.5% of the total increase in COE, whilst the capital cost (total overnight costs) for the capture system and compression train account for almost 27.3% of the cost increase. The initial and replenishment costs for the solid sorbent account for 8.4%, which is based on an attrition rate of 0.005% per cycle. This rate is estimated from that of a standard FCC catalyst obtained by a private communication with ADA-ES. The estimated costs for CO_2 transport, storage, and monitoring occupy about 5.8%.

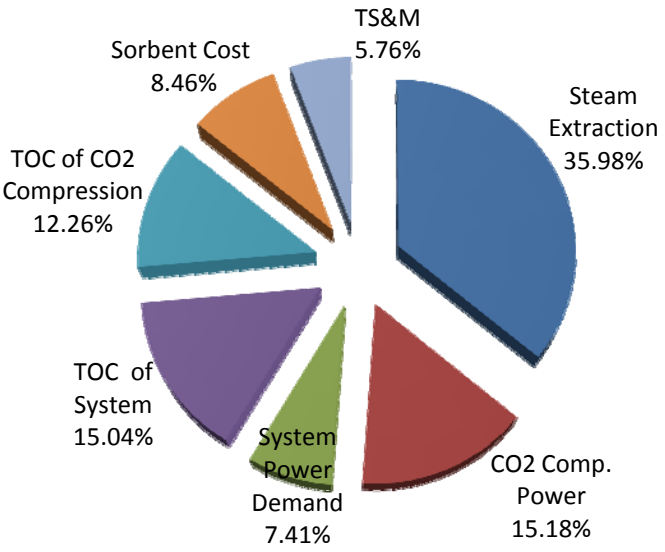

Figure 6-1. Cost contributions to COE increase

The single most significant contributor to the increase in COE is the extraction of steam to serve as a heat source for regeneration. In this process, 379.7 lb/s of steam is extracted at the LP/IP crossover of the turbine cycle, which is equates to a derating of 159.62 MWe. Investigating the enthalpy flows for the primary heat sources and sinks in the regenerator, This process achieves a working capacity of approximately 1.8 mol CO_2/kg sorbent and 0.65 mole H_2O/kg sorbent.

Table 6-1, shows that 62% of the heat from this steam is used for offsetting the endothermic desorption heat (latent heat) and the remainder is necessary to increase temperature of sorbent to about 150°C (sensible heat). This process achieves a working capacity of approximately 1.8 mol CO_2/kg sorbent and 0.65 mole H_2O/kg sorbent.

Table 6-1. Enthalpy flows in adsorber and regenerator

Enthalpy Flow in 1 ADS (GJ/hr)	
Reaction	-60.96
Bicarbonate	-1.20
Carbamate	-47.10
Water	-12.67
ΔT (Sorbent)	-36.59
Cooling Water	85.40

Enthalpy Flow in 1 RGN (GJ/hr)	
Reaction	85.35
Bicarbonate	1.68
Carbamate	65.93
Water	17.74
ΔT (Sorbent)	52.77
Steam (100 psia)	-132.65

The energy required for regenerating the sorbent is compared with that of a typical amine solvent scrubbing in Table 6-2. Examples of process calculations for MEA solvent processes are obtained from Tarka et al. [9], Oyenekan [10] and the CCSI benchmark MEA process. The heat of reaction (Q_Rxn) is the energy required to drive the chemical desorption. For the aqueous amine process, this is equal to the heat of absorption of the absorber CO_2, whilst for the sorbent process this also includes the effects of water adsorbed onto the sorbent through physisorption and chemical interactions with the adsorber CO_2. For the aqueous amine process, water is vaporized in the reboiler of the regenerator column, which requires additional heat represented by the heat of vaporization term (Q_Vap). The sensible heat (Q_Sen) is the amount of energy required to heat the incoming solvent or sorbent to the regenerator temperature, and is equal to the difference in thermal energy of solvent or sorbent between inlet and outlet.

Table 6-2. Comparison of regeneration energy

	Solid Sorbent	MEA (Oyenekan)	MEA (Tarka)	MEA (CCSI)
Q_Rxn (GJ/tonne CO2)	1.82	1.48	1.90	2.18
Bicarbonate	0.04	-	-	
Carbamate	1.41	-	-	
Water	0.38	-	-	
Q_Vap (GJ/tonne CO2)	0	0.61	0.67	1.01
Q_Sen (GJ/tonne CO2)	0.97	1.35	1.91	0.61
Total Q	2.79	3.44	4.48	3.80

From Table 6-2, this solid sorbent process can be seen to have lower energy penalty for regeneration than any of the aqueous amine processes. The primary heat of reaction for CO_2 desorption, via the carbamate reaction, is not significantly different from the heat of desorbtion for the Oyenekan process; however, the low heat of desorption for water compared to heat of vaporization for water and the low specific heat capacity of the solid sorbent results in a reduction in the overall energy requirement for the sorbent system. Accordingly, the amount of steam that needs to be withdrawn from the power plant turbines to operate the regenerator should be lower for the solid sorbent process. However, the parasitic energy requirement will also depend on the pressure and temperature requirements of the steam. For example, the CCSI MEA process only requires steam at 35 psia, so it has a lower parasitic power requirement for the same mass flow of steam.

7.0 Conclusions

A set of tools and models for the synthesis and design of solid sorbent based carbon capture processes have been developed and used to develop and optimize an initial full scale design (A650.1) of a solid sorbent capture system for a 650 MWe,net (before capture) supercritical pulverized coal (PC) power plant. This process achieves 90% capture of the CO_2 emissions from a typical 650 MWe,net supercritical PC plant. The process achieves a working capacity of approximately 1.8 mol CO_2/kg sorbent and 0.65 mole H_2O/kg sorbent. Analysis of the results reveals that steam extraction is the largest contributor to the increase in COE. Compared with current aqueous amine scrubbing technology this sorbent process shows a significant reduction in the heat required for regeneration.

8.0 Glossary

Acronym	Descriptive Name
ACM	Aspen Custom Modeler
ADS	Adsorber
ARRA	American Recovery and Reinvestment Act of 2009
CCS	Carbon Capture and Storage
CCSI	Carbon Capture Simulation Initiative
CO_2	Carbon Dioxide
COE	Cost of Electricity
CPR	Compressor or Blower
DOE	Department of Energy
ELE	Solids Elevator
FGD	Flue Gas Desulfurization
FY	Fiscal Year
GHX	Gas-Liquid Heat Exchanger (with condensation)
H_2O	Water
IAB	Industry Advisory Board
ICP	Industrially-relevant Challenge Problem(s)
MW	Megawatt Thermal
MWe	Megawatt Electric
N_2	Nitrogen
NETL	National Energy Technology Laboratory
NSGA-II	Non-Dominated Sorting Genetic Algorithm II
O&M	Operation and Maintenance
ORD	Office of Research and Development
ORISE	Oak Ridge Institute for Science and Education
PC	Pulverized Coal
PEI	Polyethyleneimine
RGN	Regenerator
ROM	Reduced Order Model
SHX	Solid-Liquid Heat Exchanger
TOC	Total Overnight Cost
V	Version (For Example: V2 refers to Version 2)

9.0 References

1. Haslbeck, J.L., et al., *Cost and Performance Baseline for Fossil Energy Plants. Volume 1: Bituminous Coal and Natural Gas to Electricity*. 2010, DOE/NETL.
2. Lee, A., et al. *A Model for the Adsorption Kinetics of CO_2 on Amine-Impregnated Mesoporous Sorbents in the Presence of Water*. in *28th International Pittsburgh Coal Conference*. 2011. Pittsburgh.
3. Knaebel, K.S., *Temperature Swing Adsorption System*. 2005: United States.
4. Aungier, R.H., *Centrifugal Compressors: A Strategy for Aerodynamic Design and Analysis*. 2000, New York: ASME Press.
5. Seider, W.D., et al., *Product and Process Design Principles: Synthesis, Analysis and Evaluation*. 3rd Edition ed. 2009, Hoboken, N.J.: John Wiley and Sons.
6. Eslick, J.C. and D.C. Miller, *A multi-objective analysis for the retrofit of a pulverized coal power plant with a CO2 capture and compression process.* Computers & Chemical Engineering, 2011. **35**(8): p. 1488-1500.
7. Deb, K., et al., *A Fast and Elitist Multi-Objective Genetic Algorithm: NSGA-II.* IEEE Transactions on Evolutionary Computation, 2002. **6**(2): p. 182-197.
8. Black, J.B., et al., *Cost and Performance of PC and IGCC Plants for a Range of Carbon Dioixide Capture*, K. Gerdes, Editor. 2011, DOE/NETL.
9. Thomas, J.T., et al., *CO2 capture systems using amine enhanced solid sorbents*. 2006: Alexandria, VA, USA. p. 30.
10. Oyenekan, B.A., *Modeling of strippers for carbon dioxide capture by aqueous amines*, in *Chemical Engineering*. 2007, University of Texas at Austin: Austin, TX.
11. Kunii, D. and O. Levenspiel, *Fluidization Engineering*. 2nd Edition ed. Series in Chemical Engineering, ed. H. Brenner. 1991, Boston: Butterworth-Heinemann.
12. Ruthven, D.M., *Principles of adsorption and adsorption processes*. 1984: Wiley-Interscience.
13. Mebane, D.S., D.J. Fauth, and M.L. Gray, *A Rigorous Yet Scalable Kinetic Model for the Uptake of CO2 by Silica-Supported, PEI-Impregnated Sorbents*, in *Pittsburgh Coal Conference*. 2011.
14. Farooq, S. and D.M. Ruthven, *Heat effects in adsorption column dynamics. 2. Experimental validation of the one-dimensional model.* Ind. Eng. Chem. Res., 1990. **29**(6): p. 1084-1090.
15. Yang, R.T., *Gas separation by adsorption processes*. 1997: Imperial College Press.
16. Yoon, S.M. and D. Kunii, *Gas Flow and Pressure Drop through Moving Beds.* Ind. Eng. Chem. Proc. Des. Dev., 1970. **9**(4): p. 559-565.
17. Dixon, A.G. and D.L. Cresswell, *Theoretical prediction of effective heat transfer parameters in packed beds.* AIChE Journal, 1979. **25**(4): p. 663-676.
18. Hsu, C.T., P. Cheng, and K.W. Wong, *Modified Zehner-Schlunder models for stagnant thermal conductivity of porous media.* International Journal of Heat and Mass Transfer, 1994. **37**(17): p. 2751-2759.

Appendix A: Bubbling Fluidized Bed Reactor Model

The bubbling fluidized bed reactor model was developed based on the work of Kunii and Levenspiel [11], who developed a model for the heat and mass transfer behavior in fluidized bed reactors based on the characteristics of the bubbles rising through the bed. The model is one dimensional, considering only variations that occur in the axial (vertical) direction of the bed. Thus, the model does not consider any variations that may occur in the lateral directions due to maldistribution of gas and solids, wall effects, feed locations, etc. Inclusion of these effects would significantly increase the complexity of the model, and this level of detail is best left to the CFD models being developed by Task Set 2.

The bubbling fluidized bed reactor model divides the bed into three distinct hydrodynamic regions which coexist within the bed as shown in Figure A-1. These regions are:

1. A bubble region, representing the bubbles of gas rising through the fluidized bed,
2. A cloud-wake region, representing the cloud of gas and solids surrounding each rising bubble and carried upwards through the bed by the bubble, and
3. An emulsion region, representing the bulk of the fluidized bed.

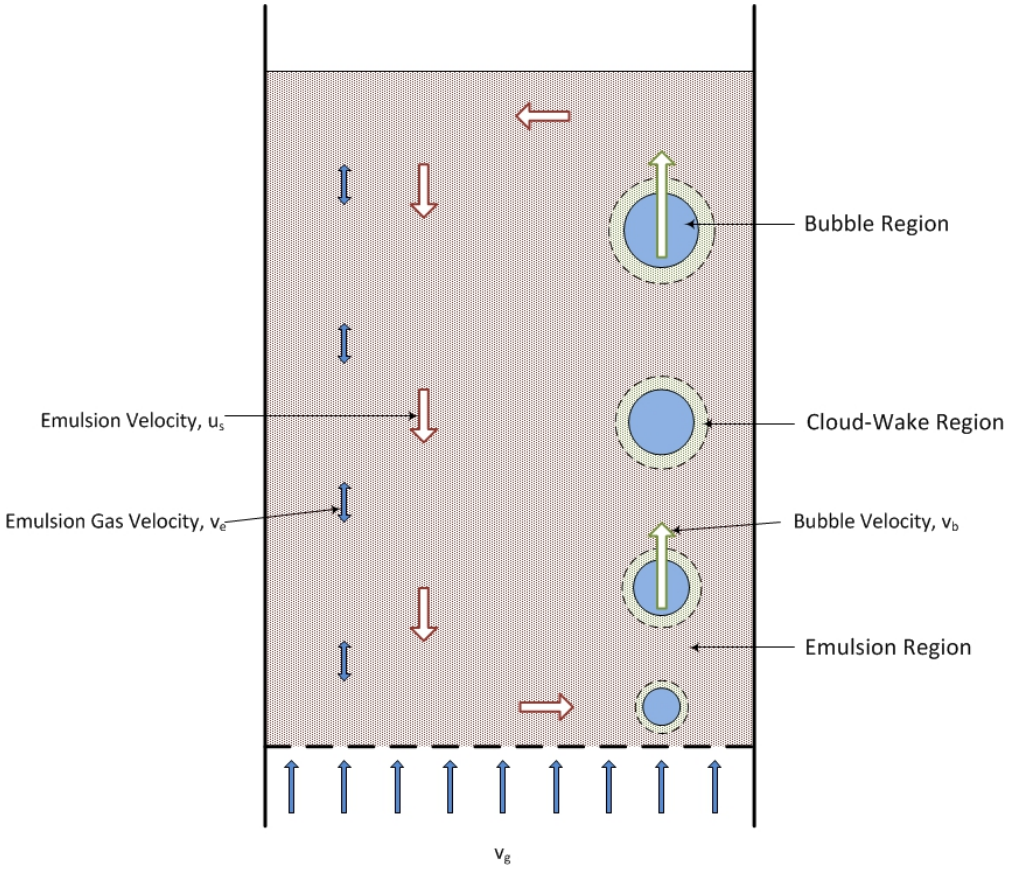

Figure A-1. Diagram showing interaction between different regions in a bubbling fluidized bed.

Each region may contain both gas and solids, and the volume fraction of solids in each region is determined separately. Heat and mass transfer occurs both between contacting regions (bubble to cloud-wake and cloud-wake to emulsion) and between gas and solids within each region. The bed is further discretized into “slices” along the axial domain, with each slice sub-divided into the three regions

discussed above. Within each slice, regions are assumed to be well mixed, and thus can be characterized by a single set of average states (temperature, pressure, concentrations, etc.). Flows of heat and mass between slices are determined by the axial velocities of the gas and solids, which are calculated using hydrodynamic correlations. Flows between regions within a slice are determined by heat and mass transfer correlations, as shown in Figure A-2.

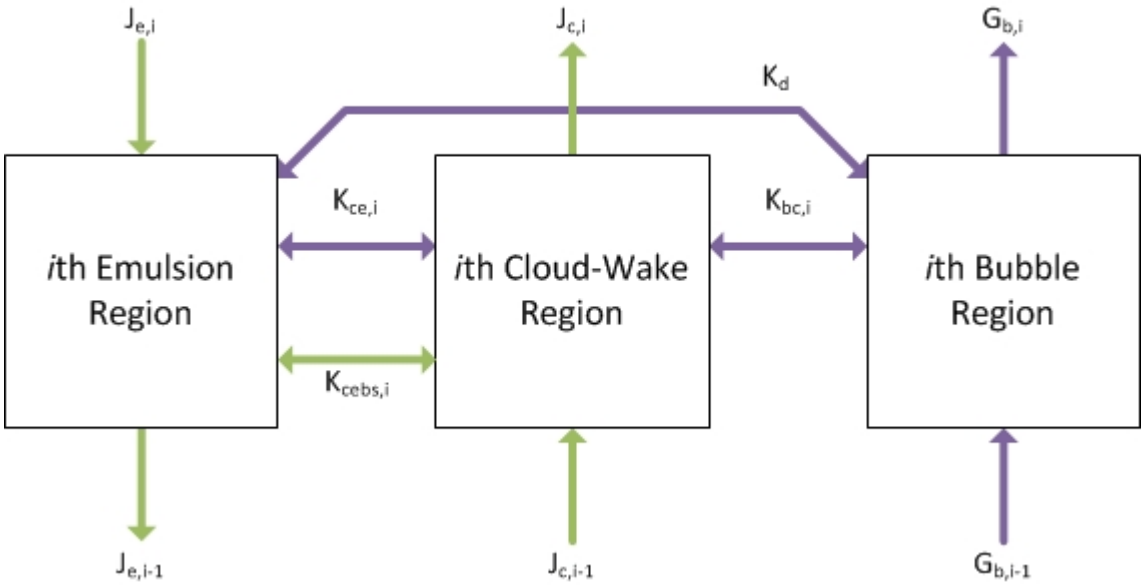

Figure A-2. Flow diagram for an arbitrary slice within the bed.

The model also includes correlations for the transfer of heat to and from objects immersed within the fluidized bed to account for the presence of heat exchangers. These are necessary to control the temperature of the fluidized bed due to the highly exothermic nature of the adsorption reactions.

Assumptions

- Bubbles contain no solids – it is assumed that the bubble region contains no solids, and thus that no reaction or gas-solids heat and mass transfer occurs in this region. Experimental evidence shows that the solids volume fraction within the bubbles of a bubbling fluidized bed in extremely low (on the order of 0.001)
- Negligible axial flow of gas in cloud-wake and emulsion regions – it is assumed that most of the axial flow of gas occurs through the rising bubbles in the bubble region, and that the axial flow of gas through the other two regions is negligible in comparison.
- Axial diffusion is negligible – it is assumed that diffusion of gas in the axial direction is negligible in comparison to the bulk flow of gas, and can thus be neglected.
- Pressure drop across reactor consists of only the static head of the fluidized solids and the pressure drop across the distributor plate – all other pressure losses in the system are negligible in comparison.

- Enthalpy of gaseous species adsorbed by solids is exactly equal to the enthalpy of the adsorbed species formed – this assumption is necessary due to lack of information on the heats of formation and specific heat capacities of the adsorbed species.
- Uniform temperature within solid particles – the model does not consider temperature gradients within individual solid particles.
- Constant solids properties – it is assumed that the properties of the solid sorbent remain constant within the fluidized bed. This neglects the effects of attrition which will affect the particle size of the sorbent, as well as any changes to the density or thermal properties of the sorbent due to the adsorption of species from the gas.
- Particles characterized by surface area mean diameter – it is assumed that the hydrodynamic characteristics of the bulk solid sorbent can be accurately represented using the surface area mean particle diameter. For sorbent particles with a narrow particle size distribution, this assumption should be sufficient.
- No entrainment of solids – the bubbling fluidized bed reactor model does not currently contain correlations to determine the rate of entrainment of particles from the top of the bed. Thus, the model assumes that entrainment is negligible and does not consider any reactions that may take place in the freeboard of the vessel.
- Single pass, vertical internal heat exchanger tubes in a square pitch arrangement.
- Negligible pressure drop and thermal resistance in heat exchanger tubes.

Model Equations

The bubbling fluidized bed reactor models consists of a large set of coupled partial differential and algebraic equations which must be solve simultaneously. The main equations in the model are listed below, and must be solved for each discretized slice in the model.

1. Mass and energy balances for each phase and region.
2. Empirical correlation for the formation and rate of growth of bubbles within the bed.
3. Empirical correlation for the rising velocity of gas bubbles based on their size.
4. Calculation of pressure drop in the bed.
5. Calculation of physical properties of gas phase using a commercial package (Aspen Properties or Multiflash).
6. Correlations for heat and mass transfer coefficients based on bubble size and velocity.
7. Empirical correlation for heat transfer to immersed objects in bed (heat exchanger tubes).
8. Empirical correlation for reaction rates (see below).

Kinetic Model

The bubbling fluidized bed reactor model uses the lumped parameter kinetic model developed by Task Set 1 for the NETL32D sorbent to calculate reaction rates within the bed. The lumped parameter model considers both adsorption and desorption reactions and can determine equilibrium conditions between gas and solids. The lumped parameter kinetic model considers three potential adsorption mechanisms that are likely to occur within a solid sorbent based carbon capture process:

1. Uptake of water by physisorption,
2. Uptake of CO_2 by the formation of bicarbonate in the presence of water, and
3. Uptake of CO_2 by the formation of carbamate ions.

Reaction rates for each reaction are calculated locally for each discretized region of the fluidized bed using the calculated local gas concentrations and solid loadings, thus the reaction rate and equilibrium conditions van vary throughout the bed. As discussed earlier, each discretized region is assumed to be well mixed, thus the average gas concentration and solid loadings are used to calculate the reaction rates. The lumped parameter kinetic model is also used to determine the heat of reaction due to adsorption and desorption, and thus the amount of heat generated or consumed by the reactions.

Appendix B: Moving Bed Reactor Model

Moving bed reactors of solid particle have been applied in several gas-solid contacting processes in the metallurgical, chemical, and petroleum industries. However, only a few investigations have been carried out on the pattern of gas flow through moving beds, notwithstanding extensive studies in the field of fixed beds. So, it is commonly assumed that moving beds have transport properties similar to those of fixed beds. In general in a moving bed, contiguous solid particles move downwards under the influence of gravity, contacting a fluid in countercurrent manner, while the corresponding chemical reaction occurs. In this study, we assumed a vertical shell and tube type reactor and that gas-solid contacting takes place in the shell side and the reactor temperature is controlled by heat transfer with immersed tubes. The solid particles passed over a distributor at the top to fall onto a series of perforated trays. The perforated trays are assumed to prevent a maldistribution of solid particles and to retard particle velocity to reduce attrition and increase their residence time. Gases enter the reactor through the perforated distributor pipe at the bottom. The following figure shows a schematic of the reactor.

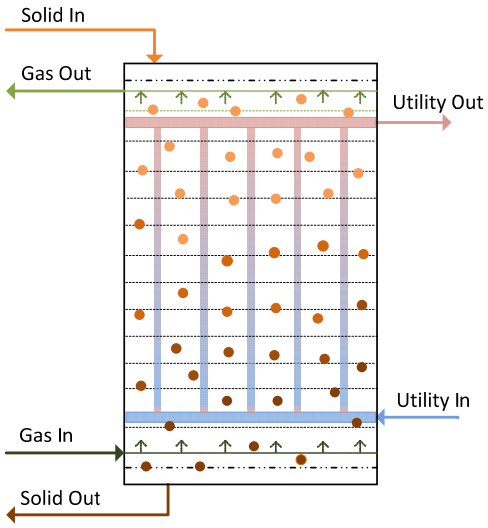

Figure B-1. Schematic diagram of moving bed reactor.

The two-phase model is used to describe heat and mass transfer between fluid and solid particles. This model comprises the mass and energy balance equations applied to both fluid and solid phases and requires constitutive equations for the mass and heat transfer between these two phases, the reaction kinetics and the equilibrium loading on the solid particle. Fluid movement is modeled by convective gas movement with axial dispersion, and counter-current solid plug flow. The LDF (Linear Driving Force) approximation is used to describe the reaction kinetics. Coefficients are estimated by the correlation based on the combination of intra-particle diffusion and film resistances to mass transfer.

Assumptions

- Vertical shell & tubes type reactor
  - Shell-side: Reactive gas & solid
  - Tube-side: Heat exchanging medium
- The system is represented as one dimensional PDEs in the axial direction
  - Gas movement can be approximated as plug flow with axial dispersion
  - Solid movement can be approximated as uniform flow with constant velocity

        - Particles are uniformly dispersed through the reactor with constant voidage
- The reactor is fully mixed in the radial direction
    - Imaginary internals (e.g. plates) are assumed for solid distribution
        - Particle flow through column plates is unrestricted
        - Gas pressure drop across plates is negligible
- Ergun equation represents pressure drop through bed
- Uniform solids temperature (no temperature profile within particles)
- Linear Driving Force approximation is used for mass transfer
- Empirical correlations for dimensionless numbers
- Ignore effects of particle attrition
- Velocity remains well below transition velocity
- Three components in each gas and solid phase
    - CO_2, H_2O and N_2 in the gas phase.
    - Bicarbonate, carbamate and physisorbed water on the solid phase.

Model Equations

The moving bed reactor models consists of a large set of coupled partial differential and algebraic equations which must be solve simultaneously. The main equations to be solved for each discretized slice in the model are presented below.

Calculation of Physical Properties

A number of physical properties of the fluids used within the model are calculated using commercial property package. Properties are also calculated for each axial slice of the model, and the properties currently calculated are follows:

- Molar density of gas in gas phase
- Molar heat capacity of gas in gas phase
- Viscosity of gas in gas phase
- Thermal conductivity of gas in gas phase
- Diffusivity of gas in gas phase
- Average molecular weight of gas in gas phase
- Molar heat capacity of adsorbed gas in solid phase
- Molar density of heat exchanger fluids
- Molar enthalpies of heat exchanger fluids

Additionally, the heat capacity and dew (saturation) temperature of heat exchanger fluid should be obtained when steam is used as the heat exchanger fluid for regenerator.

Mass Balance Equations

Gas and solid flows through a moving bed can be generally represented by the axial dispersed plug flow model.

In the gas phase,

$$\varepsilon_b D_z \frac{\partial^2 C_i}{\partial z^2} - \frac{\partial (v_g C_i)}{\partial z} - (1-\varepsilon_b) \sum_j \nu_{i,j}\, \rho_s \frac{\partial Q_j}{\partial t} = 0$$

with the boundary condition, $v_g(0) C_i(0) = v_{g,0} C_{0,i}, D_z \frac{\partial C_i}{\partial z}\Big|_{z=0} = D_z \frac{\partial C_i}{\partial z}\Big|_{z=L} = 0$

When the adsorption within porous particle is sufficiently strong and fluids are at low Reynolds number regime, the Peclet number for calculating an effective axial dispersion coefficient is obtained by Wakao's suggestion [12].

$$\frac{1}{Pe'} = \frac{D_z}{v d_p} = \frac{20}{ReSc} + \frac{1}{2}$$

In the solid phase,

$$J_s \frac{\partial w_j}{\partial z} + (1 - \varepsilon_b)\rho_s \frac{\partial Q_j}{\partial t} = 0$$

with the boundary condition, $w_j(L) = w_{L,j}$

Mass Transfer

The reaction kinetics equations are represented by a linear driving force approximation as follows.

$$\rho_s \frac{\partial Q_j}{\partial t} = k_{LDF,j} a_s \left(w_j^* - w_j\right)$$

In adsorption and desorption, the mass transfer mechanism generally consists of three steps:

1. Fluid film transfer
2. Pore diffusion
3. Surface diffusion

Adsorbent initially transfers from the bulk gas phase through an external film to the external surface of the particles. The molecules are diffused into the pores of the particle, adsorbed on the active sites and then diffused along the surface. While fluid film transfer and pore diffusion are treated as sequential steps, pore diffusion and surface diffusion generally occur in parallel. Any combination of the three steps can constitute the rate-controlling mechanism. This mechanism definitely depends on the adsorption system and can vary with the operating conditions of the process.

According to Mebane et al. [13], gas diffusion is considered to be infinitely fast and Knudsen diffusion takes place at the intermediate length scale, while solid-state diffusion takes place at the smallest length scale for diffusion of CO_2 in mesoporous silica-supported polyethyleneimine (PEI) sorbents. It is in fact more convenient to depict various transfer rates in terms of an effective transfer coefficient or a lumped resistance coefficient rather than to use a diffusion equation to represent adsorption kinetics in a rigorous manner. For the adsorption and desorption of gases in mesoporous particles, the effective mass transfer coefficient can be written as the follows [14]:

$$\frac{1}{k_{LDF,j} a_s} = \frac{w_{0,j}^*}{\sum_i \gamma_{j,i} C_{0,i}} \left(\frac{1}{k_{f,j} a_s} + \frac{d_p^2/4}{15 D_{e,j}}\right)$$

It is known that the appropriate dimensionless number characterizing the film mass transfer is Sherwood number and many correlations have been developed by fitting the experimental data. These have been reviewed by Wakao and Funazkri who reanalyzed most of available experimental data and pointed out an error made in most previous correlations [12]. Consequently, the external film mass transfer coefficient is obtained by the follow equation.

$$Sh \equiv \frac{d_p k_{f,j}}{\sum_i \gamma_{j,i} D_{g,j}} = 2.0 + 1.1 Sc^{1/3} {Re_p}^{0.6}$$

For the present model, the effective diffusivity is assumed by the below simple empirical method based on Knudsen diffusion, since not much is known about the solid-state diffusion of CO_2 in PEI sorbent.

$$D_{e,i} = \frac{\alpha D_{k,i}}{\tau}$$

The Knudsen diffusivity is [15]

$$D_{k,i} = \frac{d_p}{3}\left(\frac{8RT}{\pi M}\right)^{\frac{1}{2}} = 9.7 \times 10^3 \frac{d_p}{2}\left(\frac{T}{M}\right)^{\frac{1}{2}}$$

Momentum Balance (Pressure Drop)

Yoon and Kunii [16] suggested that the Ergun equation, well-known correlations of pressure drop for fixed beds, can be applied to moving beds using the slip velocity. Absolute slip velocity is used in the follow equation with positive fluid velocity being upward and positive particle velocity being downward.

$$\frac{\partial P}{\partial z} = -\left\{\frac{150\times10^{-5}\mu_g(1-\varepsilon_b)^2}{(d_p\psi)^2\varepsilon_b^3}\varepsilon_b\left(\frac{v_g}{\varepsilon_b}+\frac{v_s}{1-\varepsilon_b}\right) + \frac{1.75\times10^{-5}\rho_g(1-\varepsilon_b)}{(d_p\psi)\varepsilon_b^3}\varepsilon_b{}^2\left(\frac{v_g}{\varepsilon_b}+\frac{v_s}{1-\varepsilon_b}\right)^2\right\}$$

Energy Balance Equation

For a non-isothermal reactor, the differential energy balance for both phases may be written as follows:

In the gas phase,

$$\varepsilon_b k_g \frac{\partial^2 T_g}{\partial z^2} - C_{p,g} v_g \rho_g \frac{\partial T_g}{\partial z} - P\frac{\partial v_g}{\partial z} + (1-\varepsilon_b)h_{gs}a_s\left(T_s - T_g\right) + \left(1-\sqrt{1-\varepsilon_b}\right)h_{wg}a_w\left(T_w - T_g\right) = 0$$

with the boundary condition, $T_g(0) = T_{g,0}, k_g \frac{\partial T_g}{\partial z}\Big|_{z=0} = k_g \frac{\partial T_g}{\partial z}\Big|_{z=L} = 0$

In the solid phase,

$$C_{p,s}J_s\frac{\partial T_s}{\partial z} - (1-\varepsilon_b)h_{gs}a_s\left(T_s - T_g\right) + \sqrt{1-\varepsilon_b}h_{ws}a_w(T_w - T_s) + \sum_j \Delta H_{rxn,j}\rho_s\frac{\partial Q_j}{\partial t} = 0$$

with the boundary condition, $T_g(L) = T_{g,L}$

Under the assumption that there is no heat transfer along the tube wall, the energy balance equation on the tube-wall can be written as follows:

$$h_t a_w(T_t - T_w) - \left(1-\sqrt{1-\varepsilon_b}\right)h_{wg}a_w\left(T_w - T_g\right) - \sqrt{1-\varepsilon_b}h_{ws}a_w\left(T_w - T_g\right) = 0$$

For the adsorption, when the cooling medium constantly passes through tubes in the same direction with gas, the energy balance for tube-side is presented in Eq. (1); if the saturated steam is used to provide the heat required for regenerating the sorbent, the balance equation can be written as Eq. (2).

$$-v_t C_{p,t}\rho_t\frac{\partial T_t}{\partial z} - h_t a_w(T_t - T_w) = 0 \qquad (1)$$

$$v_t \Delta H_{vap}\frac{\partial vf}{\partial z} - h_t a_w(T_t - T_w) = 0 \qquad (2)$$

Heat Transfer Coefficient

In this study, heat transfer phenomenon in the moving-bed is modeled by correlations that have been developed for packed-bed systems, since there are few studies of the heat transfer in the moving-bed reactor. The interstitial h_{gs}, wall-to-gas h_{wg}, wall-to-solid h_{ws} heat transfer coefficients are obtained from the following correlations [12, 17]:

$$Nu = \frac{h_{gs}d_p}{k_g} = 2 + 1.1Pr^{1/3}Re_p^{0.6}$$

$$Nu_{wg} = \frac{h_{wg} d_p}{k_g} = 0.6 Pr^{\frac{1}{3}} Re_p^{0.5}$$

$$Nu_{ws} = \frac{h_{ws} d_p}{k_{sf}} = 2.12$$

where, we assumed that k_{sf} is the radial thermal conductivity of solid phase, which is given by the following equations [18]. The term, k_{sf} means an equivalent thermal conductivity of composite layer consisting of both fluid and solid phase which was introduced to reflect the effect of heat conduction of solids on the effective heat conductivity in Zehner and Schlunder's point contact model.

$$\frac{k_{sf}}{k_g} = \frac{2}{1-\lambda B}\left[\frac{(1-\lambda)B}{(1-\lambda B)^2}\ln\frac{1}{\lambda B} - \frac{B+1}{2} - \frac{B-1}{1-\lambda B}\right], \quad \lambda = \frac{k_g}{k_s}, \quad B = C\left(\frac{1-\phi}{\phi}\right)^m$$

Appendix C: Costing Methodology and Models

In this study, a 650 MWe,net (before capture) supercritical PC power plant was selected for the reference based on recent NETL studies suggesting the approximate size and type of plant suitable for retrofitting with carbon capture. The economic performance characteristics for the retrofit were investigated by cost of electricity (COE) on 2007 basis. The COE is the revenue received by the generator per net megawatt-hour during the power plant's first year of operation, *assuming that the COE escalates thereafter at a nominal annual rate equal to the general inflation rate, i.e., that it remains constant in real terms over the operational period of the power plant* [8]. According to recent NETL studies, the following simplified equation was used to estimate COE as a function of total overnight cost (TOC), fixed operation and maintenance (O&M) costs, variable O&M (including fuel) costs, annual net megawatt-hours of power (MWh) that is generated at 100 percent capacity factor.

$$COE = \frac{(CCF)(TOC) + OC_{FIX} + (CF)(OC_{VAR})}{(CF)(MWh)} + COE_{TS\&M}$$

where, CCF means the capital charge factor that matches the applicable finance structure and capital expenditure period, CF is the plant capacity factor, assumed to be constant over the operational period. $COE_{TS\&M}$ represents a COE increment converted from the capital and operating costs for CO_2 transport, storage and monitoring, which is independently estimated by the factor, f_{COE} that is extrapolated from NETL studies. In this study, two economic variables are assumed as 0.124, 0.85 for CCF, CF, respectively [8].

Total overnight cost (TOC) is calculated as the summation of reference power plant, carbon capture system and CO_2 compression system. TOC of the reference plant is obtained based on recent NETL studies by the extrapolation using net output [1, 8] and TOC of compression system is calculated by multiplying the unit cost and total required power. TOC of carbon capture system consists of initial sorbent cost and total capital investment. The former cost is obtained by the required quantity for initial reservoir and assumed sorbent cost; the latter cost is summation of f.o.b. purchase costs of each piece of major equipments multiplied by Lang factor and delivery factor. All the purchase costs for major equipments are estimated by Seider et al. [5]. The purchase cost of equipment is generally obtained from charts, equations, or quotes from vendors; however these costs are not static because of economic inflation. So, an estimate of the purchase cost at a later date is calculated by multiplying the cost from an earlier date by the ratio of a cost index. In this study, we used "The Chemical Engineering (CE) Plant Cost Index" that is published in each monthly issue of the magazine *Chemical Engineering*.

$$TOC_{Ref}[650MW, 2007yr] = TOC_{Ref}[550MW, 2007yr] \times \frac{650MW}{P_{net,ref}}$$

$$TOC_{Comp}[650MW, 2007yr] = C_{Comp} \times W_{Comp}$$

$$TOC_{CC}[650MW, 2007yr] = IC_{Sor} + C_{TCI}, \qquad C_{TCI} = f_D f_L \sum_i \left(\frac{I_{2007}}{I_b}\right) C_{p,i}$$

The fixed operation and maintenance (O&M) costs are independent expenses of whether the power generation is inactive or operating at full capacity. These costs include:

1. Operating Labor Cost
2. Maintenance Labor Cost
3. Administrative & Support Labor Cost

4. Property Taxes & Insurance

Firstly, operating labor cost is determined based on of the required number of operators (16.3 jobs/plant) and the average base labor rate ($34.65/hour) with the associated labor burden (30%). The data used to determine annual cost was taken from a recent NETL study [8]. Secondly, maintenance labor cost was estimated on the basis of relationships to initial capital cost in recent NETL studies. Administrative and support labor costs are assessed at rate of 25 percent of the burdened O&M labor costs. Property taxes and insurance cost was included as 2 percent of the total plant cost (TPC) in recent NETL study.

$$OC_{OL} = N_{op} \times C_{labor} \times Time_{op} \times (1 + f_{Labor})$$

$$OC_{ML} = f_{ML} \times TOC$$

$$OC_{ASL} = 0.25 \times (OC_{OL} + OC_{ML})$$

$$OC_{TI} = f_{TI} \times TOC$$

The variable O&M cost which is proportional to power generation consists of the followings:

1. Maintenance Material Cost
2. Consumables
3. Waste Disposal

The maintenance material cost is calculated in the same way as maintenance labor cost. The cost of consumables, including fuel, is determined on the basis of daily rates of consumption, the unit cost of each specific consumable commodity, and the plant annual operating hours. The daily rates for most consumables except limestone are evaluated on the basis of the quantity extrapolating from reference plant data based on net output power. The daily rate for limestone is obtained from the power plant model developed in Thermoflex. Quantities for sorbent make-up and additional cooling water are directly taken from process simulation and process water use is calculated by Equation 3-12. The cost for making up for sorbent loss is calculated by multiplying quantity of sorbent, annual number of cycles, loss fraction and unit cost. Waste quantities and disposal costs are determined similarly to the consumables. The available data for the daily rates and unit costs are shown in

Table C-1, where the quantities were multiplied by the capacity factor based on a 100 percent operating basis.

$$OC_{MM} = f_{MM} \times TOC$$

$$OC_{CM} = OC_{CM,Sor} + OC_{CM,PW} + OC_{CM,CW} + \sum_i OC_{CM,i}$$

$$OC_{WD} = \sum_i OC_{WD,i} = F_{WD,ref,i} \times \frac{650MW}{P_{net,ref}} \times C_{WD,i} \times 365, i = \{flyash, ash\}$$

$$OC_{CM,i} = F_{CM,ref,i} \times \frac{650}{P_{net,ref}} \times C_{CM,i} \times 365, i = \{chemicals, fuel\}$$

$$OC_{CM,Sor} = Q_{Sor} \times N_{Cycle} \times f_{Loss} \times C_{CM,Sor}$$

$$OC_{CM,CW} = \sum_j F_{CM,CW,j} \times C_{CM,CW} \times Time_{op}$$

$$OC_{CM,PW} = \frac{F_{CM,PW}}{1000} \times \frac{1\ gallon}{8.34\ lb} \times C_{CM,CW} \times Time_{op}$$

Table C-1. Daily rates and unit costs for consumables.

Consumables	/Day	Unit Cost ($)
Sorbent (lb)		5.0
Process Water (1000 gallons)	-	1.08
Cooling Water (1000 gallons)	-	0.103
Chemicals		
MU & WT Chemical (lb)	34,009	0.17
Limestone (ton)	724	21.63
28% Ammonia (ton)	18	129.80
SCR Catalyst (m3)	0.368532526	5775.94
Waste Disposal		
Flyash (ton)	465.0529501	16.23
Bottom Ash(ton)	116.7019667	16.23
Fuel (lb)	5,005	38.19

Table C-2. Parameters for costing methodology.

CCF	Capital charge factor	0.124	
CF	Plant capacity factor	0.85	
f_{COE}	Factor of calculating the COE increment for CO2 transport, storage and monitoring	0.002542	$\$/lb\ CO_2$
$P_{net,ref}$	Net output of reference plant in NETL report	550	MW
C_{Comp}	Unit price for CO2 compression system	700	$\$/hp$
f_D	Delivery factor for power plant with CO2 capture	1.05	
f_L	Lang factor for power plant with CO2 capture	5.04	
I_{2007}	CE Plant Cost Index for 2007	527	
I_b	CE Plant Cost Index for the base year, 2006	500	
N_{op}	Number of total operating jobs	16.3	
C_{labor}	Operating labor rate	34.65	$\$/hr$
$Time_{op}$	Annual operating hours	8760	hr
f_{Labor}	Factor for operating labor burden	0.3	
f_{ML}	Factor for maintenance labor cost	0.0053343	
f_{TI}	Factor for property taxes and insurance cost	0.0163	
f_{MM}	Factor for maintenance material cost	0.0080021	
f_{Loss}	Loss fraction of sorbent	0.00005	$/cycle$

Table C-3. Variables for costing methodology.

TOC_{Ref}	TOC of 650MW power plant without CO2 capture	$
TOC_{Comp}	TOC of CO2 compression system	$
TOC_{CC}	TOC of carbon capture system	$
W_{Comp}	Required power for CO2 compression	hp
IC_{Sor}	Initial cost of sorbent	$
C_{TCI}	Total capital investment	$
$C_{p,i}$	Purchase cost for each equipment	$
OC_{OL}	Annual operating labor cost	$\$/yr$
OC_{ML}	Annual maintenance labor cost	$\$/yr$
OC_{ASL}	Annual administrative & support labor cost	$\$/yr$
OC_{ASL}	Annual cost for property taxes & insurance	$\$/yr$
OC_{MM}	Annual maintenance material cost	$\$/yr$
OC_{CM}	Annual cost for consumable materials	$\$/yr$
OC_{WD}	Annual cost for waste disposal	$\$/yr$
$OC_{CM,i}$	Annual cost for each material	$\$/yr$
$F_{CM,i}$	Rate for each material	$Unit/yr$
$C_{CM,i}$	Unit cost for each material	$\$/Unit$
Q_{Sor}	Quantity of sorbent reservoir	$tonne$
N_{Cycle}	Annual number of process cycles	$cycles/yr$
$OC_{WD,i}$	Annual disposal cost for each waste	$\$/yr$
$F_{WM,i}$	Rate for each waste	$Unit/yr$
$C_{WM,i}$	Unit disposal cost for each waste	$\$/Unit$

Appendix D: Specification Sheets

2-Stage Bubbling Fluidized Bed Reactor

Identification:	**Item**	Reactor			Date:	*21 Feb. 2012*
	Item No.	ADS-001				
	No. Required	14			By:	*CCSI TS3*
Function:	Adsorber					
Operation:	Continuous					
Materials Handled:						
Top Bed	*Feed*	*Product*		*Feed*	*Product*	
Quantity (kmol/hr):		5,502	Quantity (kg/hr):	424,451		
Composition:			Loading (mol/kg):			
CO_2		0.0152	*Bicarbonate*	0.1227		
H_2O		0.0196	*Carbamate*	0.2298		
N_2		0.9652	*Water*	0.5118		
Temperature (˚C):		51.57	Temperature (˚C):	118.45		
Pressure (bar):		1.00	Pressure (bar):	1.01		
Bottom Bed	*Feed*	*Product*		*Feed*	*Product*	
Quantity (kmol/hr):	6,538		Quantity (kg/hr):		424,451	
Composition:			Loading (mol/kg):			
CO_2	0.1291		*Bicarbonate*		0.2004	
H_2O	0.0587		*Carbamate*		1.9436	
N_2	0.8122		*Water*		1.0842	
Temperature (˚C):	42.88		Temperature (˚C):		53.89	
Pressure (bar):	1.29		Pressure (bar):		1.01	
Design Data:	Inside Diameter: 9.748 m Height: 17.09 m Pressure drop: 0.29 bar Material of Construction: Carbon steel (Top/Bottom) Bed Depth: 7.232/4.854 m HX Area: 1733.7/941.3 m^2 Solid Residence Time: 19.0/13.0 min.					
Utilities:	Cooling waters at 853.2 (Top) and 818.3 (Bottom) ton/hr					
Controls:	N/A					
Tolerances:	N/A					
Comments and drawings:	See Process Flow Diagram, Section 5 and Appendix A.					

Moving Bed Reactor

Identification:	**Item**	Reactor			Date:	*21 Feb. 2012*
	Item No.	RGN-001				
	No. Required	10			By:	*CCSI TS3*
Function:	Regenerator					
Operation:	Continuous					
Materials Handled:						
	Feed	*Product*		*Feed*	*Product*	
Quantity (kmol/hr):	1,132	2,537	Quantity (kg/hr):	594,231	594,231	
Composition:			Loading (mol/kg):			
CO_2	0.0000	0.4196	*Bicarbonate*	0.2004	0.1227	
H_2O	0.9999	0.5803	*Carbamate*	1.9436	0.2298	
N_2	0.0001	0.0000	*Water*	1.0842	0.5118	
Temperature (˚C):	105	72.65	Temperature (˚C):	69.16	134.66	
Pressure (bar):	1.86	1.01	Pressure (bar):	1.01	1.01	
Design Data:	Inside Diameter: 7.147 m Height: 4.592 m Pressure drop: 0.85 bar Material of Construction: Carbon steel HX Area: 1573 m^2 Average Bed Voidage: 0.609 Solid Residence Time: 3.14 min.					
Utilities:	Saturated Steam (6.89 bar) at 62,051 kg/hr					
Controls:	N/A					
Tolerances:	N/A					
Comments and drawings:	See Process Flow Diagram, Section 5 and Appendix B.					

Compressor

Identification:	**Item**	Compressor	
	Item No.	CPR-001	Date: *21 Feb. 2012*
	No. Required	See below	
			By: *CCSI TS3*

Function:	Flue gas compressor
Operation:	Continuous

Materials Handled:

	Feed	*Product*
Quantity (kmol/hr):	7,170	7,170
Composition:		
CO_2	0.1177	0.1177
H_2O	0.1417	0.1417
N_2	0.7406	0.7406
Temperature (˚C):	54.18	80.65
Pressure (bar):	1.01	1.29

Design Data:	Centrifugal Blower Type Material of Construction: Carbon steel Power Consumption: 2234.8 hp (2 units for 2000 hp and 1 unit for 234.8 hp)
Utilities:	Electricity
Controls:	N/A
Tolerances:	N/A
Comments and drawings:	See Process Flow Diagram, Section 5.

Compressor

Identification:	**Item**	Compressor	Date: *21 Feb. 2012*
	Item No.	CPR-002	
	No. Required	1	By: *CCSI TS3*
Function:	Circulating the HX fluid between SHX-001 and SHX-002		
Operation:	Continuous		
Materials Handled:			
	Feed	*Product*	
Quantity (kmol/hr):	270	270	
Composition:			
CO_2	0.0000	0.0000	
H_2O	1.0000	1.0000	
N_2	0.0000	0.0000	
Temperature (˚C):	111.35	127.89	
Pressure (bar):	1.3	1.5	
Design Data:	Centrifugal Blower Type Material of Construction: Carbon steel Power Consumption: 61.2 hp		
Utilities:	Electricity		
Controls:	N/A		
Tolerances:	N/A		
Comments and drawings:	See Process Flow Diagram, Section 5.		

Pump

Identification:	**Item**	Compressor	Date: *21 Feb. 2012*
	Item No.	CPP-002	
	No. Required	1	By: *CCSI TS3*
Function:	Circulating the HX fluid between SHX-001 and SHX-002		
Operation:	Continuous		
Materials Handled:			
	Feed	*Product*	
Quantity (kmol/hr):	270	270	
Composition:			
CO_2	0.0000	0.0000	
H_2O	1.0000	1.0000	
N_2	0.0000	0.0000	
Temperature (˚C):	111.35	111.35	
Pressure (bar):	1.3	1.5	
Design Data:	Centrifugal Pump Material of Construction: Cast steel Liquid Flowrate: 23.7 gpm Driver Power Consumption: 0.15 hp		
Utilities:	Electricity		
Controls:	N/A		
Tolerances:	N/A		
Comments and drawings:	See Process Flow Diagram, Section 5.		

Heat Exchanger

Identification:	**Item**	Gas Heat Exchanger	Date:	*21 Feb. 2012*
	Item No.	GHX-001		
	No. Required	See below	By:	*CCSI TS3*

Function:	Flue gas heat exchanger
Operation:	Continuous

Materials Handled:

Shell side - CW	*Feed*	*Product*	*Tube side - Gas*	*Feed*	*Product*
Quantity (kg/hr):	294,595	294,595	Quantity (kmol/hr):	7,170	6,538
Composition:			Composition:		
CO_2	0.0000	0.0000	CO_2	0.1177	0.1291
H_2O	1.0000	1.0000	H_2O	0.1417	0.0587
N_2	0.0000	0.0000	N_2	0.7406	0.8122
Temperature (˚C):	33	60.65	Temperature (˚C):	80.65	42.88
Pressure (bar):	1.00	1.00	Pressure (bar):	1.29	1.29

632 kmol/hr of water is condensed.

Design Data:

Floating Head Shell-and-Tube Type
Material of Construction: Stainless steel
Tube Length: 12 ft
U: 250 $W/m^2/K$
LMTD: 14.348 ˚C

HX Area: 3271.9 m^2 = 35,218.4 ft^2

(2 units for 12,000 ft^2 and 1 unit for 11,218 ft^2)

Utilities:	N/A
Controls:	N/A
Tolerances:	N/A
Comments and drawings:	See Process Flow Diagram, Section 5.

Heat Exchanger

Identification:	**Item**	Gas Heat Exchanger	Date:	*21 Feb. 2012*
	Item No.	GHX-002		
	No. Required	See below	By:	*CCSI TS3*
Function:	Product CO_2-rich gas heat exchanger			
Operation:	Continuous			

Materials Handled:

Shell side - CW	*Feed*	*Product*	*Tube side - Gas*	*Feed*	*Product*
Quantity (kg/hr):	743,599	743,599	Quantity (kmol/hr):	2,537	1,138
Composition:			Composition:		
CO_2	0.0000	0.0000	CO_2	0.4196	0.9358
H_2O	1.0000	1.0000	H_2O	0.5803	0.0641
N_2	0.0000	0.0000	N_2	0.0000	0.0001
Temperature (˚C):	33	52.65	Temperature (˚C):	72.65	40
Pressure (bar):	1.20	1.10	Pressure (bar):	1.01	1.01

1132 kmol/hr of water is condensed

Design Data:

Floating Head Shell-and-Tube Type
Material of Construction: Carbon steel
Tube Length: 12 ft
U: 250 W/m^2/K
LMTD: 12.383 ˚C

HX Area: 3271.9 m^2 = 73186.2 ft^2

(6 units for 12,000 ft^2 and 1 unit for 1,186.2 ft^2)

Utilities:	N/A
Controls:	N/A
Tolerances:	N/A
Comments and drawings:	See Process Flow Diagram, Section 5.

Heat Exchanger

Identification:	**Item**	Solid Heat Exchanger	Date:	*21 Feb. 2012*
	Item No.	SHX-001		
	No. Required	1	By:	*CCSI TS3*
Function:	Solid heat exchanger before the regenerator			
Operation:	Continuous			

Materials Handled:

Shell side – Sat. Steam	*Feed*	*Product*	*Tube side - Solids*	*Feed*	*Product*
Quantity (kmol/hr):	743,599	743,599	Quantity (kg/hr):	594,231	594,231
Composition:			Loading (mol/kg):		
CO_2	0.0000	0.0000	*Bicarbonate*	0.2004	0.2004
H_2O	1.0000	1.0000	*Carbamate*	1.9436	1.9436
N_2	0.0000	0.0000	*Water*	1.0842	1.0842
Temperature (˚C):	127.89	111.35	Temperature (˚C):	53.89	69.16
Pressure (bar):	1.5	1.3	Pressure (bar):	1.01	1.01

Design Data:	Floating Head Shell-and-Tube Type Material of Construction: Carbon steel Tube Length: 12 ft U: 300 $W/m^2/K$ LMTD: 58.090 ˚C HX Area: 207.9 m^2 = 2238.1 ft^2
Utilities:	N/A
Controls:	N/A
Tolerances:	N/A
Comments and drawings:	See Process Flow Diagram, Section 5.

Heat Exchanger

Identification:	**Item**	Solid Heat Exchanger	Date:	*21 Feb. 2012*
	Item No.	SHX-002	By:	*CCSI TS3*
	No. Required	1		

Function:	Solid heat exchanger after the regenerator
Operation:	Continuous

Materials Handled:

Shell side – Sat. Steam	*Feed*	*Product*	*Tube side - Solids*	*Feed*	*Product*
Quantity (kmol/hr):	743,599	743,599	Quantity (kg/hr):	594,231	594,231
Composition:			Loading (mol/kg):		
CO_2	0.0000	0.0000	*Bicarbonate*	0.1227	0.1227
H_2O	1.0000	1.0000	*Carbamate*	0.2298	0.2298
N_2	0.0000	0.0000	*Water*	0.5118	0.5118
Temperature (˚C):	111.35	111.35	Temperature (˚C):	134.66	118.45
Pressure (bar):	1.5	1.3	Pressure (bar):	1.01	1.01

Design Data:	Floating Head Shell-and-Tube Type Material of Construction: Carbon steel Tube Length: 12 ft U: 300 $W/m^2/K$ LMTD: 13.637 ˚C HX Area: 874.0 m^2 = 9407.4 ft^2
Utilities:	N/A
Controls:	N/A
Tolerances:	N/A
Comments and drawings:	See Process Flow Diagram, Section 5.